A Comparison of Active and Passive Cell Balancing Techniques for Series/Parallel Battery Packs

A Thesis

Presented in Partial Fulfillment of the Requirements for

the Degree Master of Science in the

Graduate School of The Ohio State University

By

James D. Welsh, Jr., B.S.

Electrical and Computer Engineering

Graduate Program

The Ohio State University

2009

Master's Examination Committee:

Prof. Stephen Yurkovich, Adviser

Prof. Yann Guezennec

Abstract

The automobile industry is progressing toward plug-in hybrid (PHEV) and fully electric vehicles (EV) in the near future. These new advanced architectures require a substantially larger battery pack, which is used as the powertrain's primary energy storage device. Larger battery packs allow these vehicles to meet the demands of greater electric ranges by using more parallel strings to increase the overall energy storage capacity of the system. The life expectancy and performance of the battery pack is of utmost importance. Due to manufacturing inconsistencies and unique performance characteristics of individual cells in a typical pack, charge balancing of a series/parallel configured battery module is critical. In this thesis, two different balancing techniques are proposed and analyzed. A passive balancing system that uses shunt resistors and an active balancing system that uses a"floating capacitor" technique are proposed and applied to a battery module with such a configuration in order to balance the individual battery cell voltages. A MATLAB simulator has been developed to model the effects of both of these balancing techniques over a series/parallel configured battery pack. This allows a thorough study of the balancing system by varying the circuit parameters to establish a trend for the effects on system performance. Additionally, the simulator provides a method for direct comparison between the two balancing techniques. Results of an experimental setup with a preliminary design of the "floating capacitor" cell balancing system are also discussed.

This is dedicated to my parents

ACKNOWLEDGMENTS

I would first like to thank my advisor, Prof. Yurkovich, for providing me with amazing support and encouragement in all of my research. In addition, I would like to thank Prof. Guezennec for helping understand the fundamentals of battery behaviors. With out their patient guidance, this research would not have been possible.

I would also like to thank B.J. Yurkovich for getting me involved in battery research as well as his extensive contributions with the numerous battery system modeling issues that arose throughout the time spent on my research. His help with the problems during the implementation of the active cell balancing system layered on the battery pack model is truly appreciated. Our many discussions along with his input on the various simulations and tests has added to the quality of the results observed. He is the best colleague I could have ever hoped for.

I would like to acknowledge the contributions of Jay Chuang in the experimental aspects of this research. Without his assistance, the experimental works of this research would have impossible. The work completed by Jay has added extensive insight to the feasibility of this active cell balancing design. The initial experimentations conducted by Jay has shown that proper shuttling can be completed with appropriately sized components. His work has also lead to the validation of the model used to generate the simulated results.

Many thanks goes out to Yiran Hu for his help with any MATLAB and LaTeX errors that occurred while completing this work. A special thanks goes to all the graduate students and advisors that I worked with on the EcoCAR team. Our discussions helped me solve many problems that I faced. Additionally, I would like to thank the EcoCAR competition for providing me financial support through the EcoCAR fellowship program.

Lastly, I would like to thank all of my friends and family for their unwavering support and motivation throughout my graduate studies. Without their continuous encouragement, this thesis would not have been possible.

VITA

July 10, 1985	Born - Cincinnati, OH, USA
2003-2007	B.S. Electrical and Computer Engineering, The Ohio State University
2008-present	Graduate Fellow

PUBLICATIONS

Research Publications

J. Welsh, B.J. Yurkovich, S. Yurkovich, Y. Guezennec. "A Floating Capacitor Cell Balancing Method for Parallel Battery Modules," *s*ubmitted to *American Control Conference*, July, 2010.

FIELDS OF STUDY

Major Field: Electrical and Computer Engineering

Contents

List of Tables

Table **Page**

List of Figures

Figure **Page**

Chapter 1

INTRODUCTION

1.1 Battery Packs

Hybrid electric vehicles (HEVs) have become the most viable and commercially available alternative to the standard internal combustion engine (ICE) vehicle. HEVs offer the benefits of reduced emissions and increased fuel economy while maintaining overall vehicle performance, as measured by metrics such as 0-60 acceleration time, braking, handling and towing. When developing a battery pack for automotive applications, several more design constraints need to be considered. The biggest effect on vehicle performance is the weight of the vehicle. Therefore, additional constraints such as size, weight and packaging also need to be optimized along with reliability, cost, performance and battery pack capacity.

The majority of HEVs currently use nickel-metal hydride (NiMH) battery packs. Vehicles such as plug-in hybrid vehicles (PHEVs) and electric vehicles (EVs) will need battery packs that have a significantly larger effective energy density in order to achieve improved emissions and fuel economy. Lithium-ion battery packs currently provide the best solution to this issue.

1.1.1 Nickel-Metal Hydride

Current production HEVs use nickel-metal hydride battery packs, which are more economically feasible than lithium-ion packs. Nickel metal hydride battery packs have many additional features that have established this technology as the energy storage system in this market. These batteries have a relatively high abuse tolerance to overcharging and overdischarging and a wide range of operating temperatures ($-30\,^{\circ}\mathrm{C}$ to $+65\,^{\circ}\mathrm{C}$). Additionally, they are relatively maintenance free and have a long cycle life (600 to 1200 cycles to 80% depth-of-discharge (DoD)) [6], as estimated from the number of battery cycles completed over a ten year span. NiMH batteries also have a higher energy density and power density than previous battery technologies, not including lithium-ion, which has made these battery packs the choice for current HEV applications.

Charge and discharge reversibility is a very important factor because a variation in symmetry at various values of state-of-charge (SoC) can result in a growth of charge imbalance or functional degradation of the individual battery cells in a pack [7]. The reversibility in NiMH packs is seen over an SoC range between 40% and 80% [8]. Below the lower bound, the internal resistance of the cells increases due to electrode and transport kinetics which reduces the available discharge power [9]; whereas above the upper bound, pressure within the cells causes the onset of hydrogen exchange which decreases the overall specific discharge power [10]. Therefore, a balance in SoC of the pack needs to be maintained so that there is sufficient discharge power for electric boost as well as sufficient headroom for energy recovery from regenerative breaking.

Current HEVs use a significantly tighter range of SoC during operation to reduce the effects of aging on a battery pack and maximize safety. The Toyota Prius is

an extreme example of this. It sustains an operating SoC of 56% while cycling SoC deviation from the nominal within a tight tolerance of 5%. Other HEVs have a greater tolerance of around 15% which, thus far, has been shown to not have any major effects on the life of the battery pack [7]. These tolerances are needed because of the relatively flat voltage curve across the 40% to 80% SoC range. The average variation is approximately 0.7 mV per percent SoC in this range, which is very difficult to manage. Maintaining such a tight tolerance can allow the pack to have a significantly longer life. The risk of the battery pack going into thermal runaway and possibly exploding is reduced, thus increasing the overall safety of the electrical system as well as the vehicle passengers.

In order to achieve a larger electrical range, the SoC deviation tolerance needs to be greater. Therefore, other chemistries such as lithium-ion are being considered, since they have a greater range of operation without the drawback of reducing the lifespan of the battery pack on board. With such a flat voltage curve along the desired range, SoC estimation and cell balancing is also more difficult with a nickel-metal hydride chemistry. Future HEVs, as well as EVs and PHEVs, will need to consider technologies that can achieve greater performance metrics.

1.1.2 Lithium-Ion

Until recently, the lithium-ion battery has only been used in small consumer electronic devices such as cell phones and computers. Due to the cost and the difficulty of the technology, until recently the lithium ion battery has not been considered practical for larger applications such as the use in advanced automotive applications. The

battery pack is considered the key element when designing alternative propulsion systems because its power and life decisively define the cost of the overall system [11]. The development of PHEVs and EVs requires larger battery packs to increase electrical capacity because of the emphasis being placed on electric range and performance. Therefore the lithium-ion battery is considered the most commercially viable option.

With the development of PHEVs and EVs, a wider range of SoC operation, which lithium-ion batteries are capable of, is needed. When compared to NiMH batteries, lithium-ion batteries offer superior advantages such as a higher cell voltage, superior energy density and a lower self-discharge rate with no memory effect [12]. To create such a battery pack, the cells are connected in series strings to increase the overall pack voltage and strings are connected in parallel to increase the overall capacity. This also increases the complexity of the system design and operation. Several issues arise as a result of this complexity in areas such as battery system safety, thermal management and battery management.

The chemical composition of lithium-ion batteries poses several health and safety hazards, which is a major concern. The high energy density that these cells possess, along with the reactive nature of the materials, make the battery system susceptible to electrolyte fire, thermal runaway and in the worst case scenario, explosion [11]. Proper safety measures such as burst disks on each cell and fire resistant trays should be used when designing these types of battery packs. The battery packs that are designed for automotive applications must also be designed with passenger safety in mind. Not only should there be safety measures if there is a failure during the operation of the system, but also in the event of a vehicle crash. Therefore the packs

must be vented to the outside of the vehicle to prevent any harmful fumes from contaminating the air of the passenger cabin.

An integral part of any lithium-ion battery pack is the thermal management system. The thermal abuse tolerance of a pack is extremely sensitive to the exothermic behavior of the cells. As the energy density of batteries increases, the exothermic behaviors become more volatile and a larger number of thermal incidents have been reported [13]. Therefore, the battery pack must maintain the rated optimal operating temperature range which is typically less than the operating temperature of the vehicle. If the batteries are not operated within this optimal range, the performance and life expectancy of the cells within the pack will be affected [14]. If the temperature is not monitored and maintained throughout the operation of the system, the cells could become electrically imbalanced [15] and overheating could occur. This would result in thermal runaway and the eventual failure of one or more battery cells in the pack.

The characteristics of lithium-ion batteries and the possible failure mode situations make a battery management system (BMS) very important in the overall lithium-ion battery pack design. Due to manufacturing inconsistencies and unique performance characteristics of the individual cells in a battery pack, the cells will charge and discharge differently during battery pack operation [16]. Therefore, cell monitoring and balancing is critical. Throughout the operation of the pack, the voltages of the individual cells will start to drift away from each other over time and an imbalance in SoC will result, causing the battery pack to operate at a lower efficiency. Particularly for a series string of cells, the full electric potential will never be realized since it will operate at the level of the weakest cell. This imbalance may cause some of the battery

cells in the pack to operate in overvoltage and undervoltage conditions, reducing the overall life expectancy of the pack. Therefore, the focus of this research will revolve around the cell balancing feature of the BMS and how the BMS can increase the performance efficiency of a battery pack.

1.2 Cell Balancing Methods

Three different cell balancing methodologies are typically employed for series strings: charging, passive and active. Active cell balancing methods remove charge from higher cells and deliver it to lower cells while passive methods remove the excess energy from the high cells through a resistive element until the charge matches those of the lower cells in the pack. Charging methods are typically only applicable to EV applications since the battery pack is usually fully charged between each use [2].

The battery pack for an HEV must be maintained at an SoC so that it can discharge the required power for a boost or launch assist while still having enough available capacity to accept all the power from regenerative braking [2]. Many battery management systems that are currently used in modern EV and PHEV applications employ a passive battery management system. The most common of these passive systems uses a resistive clamp method for balancing. Local circuits are designed around a string of cells which switch on shunt paths that divert excess charging current around fully charged cells when they reach their upper voltage limit. This resistive clamp method achieves a balancing effect where the SoC is maintained at nearly 100 percent, but also results in a significant energy loss [7], [17]. The advantage of this method is the relatively low cost and complexity, however the disadvantage is that it results in a high amount of energy loss.

Active cell balancing methods work to reduce the high energy losses observed in dissipative management systems. The next section provides a more detailed description of these types of techniques. The primary research component of this thesis will focus on developing an active cell balancing method for a battery module that consists of cells in a 3P4S (3 Parallel, 4 Series) configuration. These battery modules can then be strung together to form a larger battery pack, to meet specifications for use in automotive applications. Battery packs designed for HEVs and PHEVs must have a parallel configuration to increase the capacity of the pack to extend the electrical range of the vehicle. As mentioned before, there has been research designed around series strings. This research will use similar topologies on parallel strings with the goal of maintaining a high energy efficiency while reducing the cost and hardware complexity of the system.

1.3 Active Cell Balancing Literature Review

There are typically two different categories of active cell balancing methods: charge shuttling and energy converters [2]. Energy converters use transformers and inductors to move energy among the cells of a battery pack. A buck-boost conversion method proposed in [18] shunts each of the cells in a string with a converter. This dynamically balances all of the cells over a charging period. The results show that balancing is achieved with greater efficiency and minimal circuit losses as compared to other non-dissipative methods. Similarly, [19] uses an isolated dc-to-dc converter with a multiwinding transformer to integrate charge equalization functionality during a trickle charging period. [20] uses bi-directional dc-to-dc converters to not only balance cells during charging periods, but also discharging periods as well. The circuits

are not complex to build, however there are many electrical components needed which increases the overall cost of the system.

A variation is to use buck-boost converters in parallel with a group of battery cells that are in a series connection as shown in Figure 1.1. This reduces component overhead while providing a stable DC voltage and eliminating the charge imbalance. Therefore, cells can avoid being overcharged or overdischarged with this parallel configuration. An additional advantage to this setup is that a completely exhausted or damaged cell can be isolated or replaced without interrupting the system operation. The major drawback of this method is the total energy conversion efficiency in parallel operation may decrease, especially when the input voltage of the converter is much lower than the output voltage. Although there are several advantages to the design, the overall cost and the decrease in energy efficiency eliminate it as a possible choice for the research in this thesis.

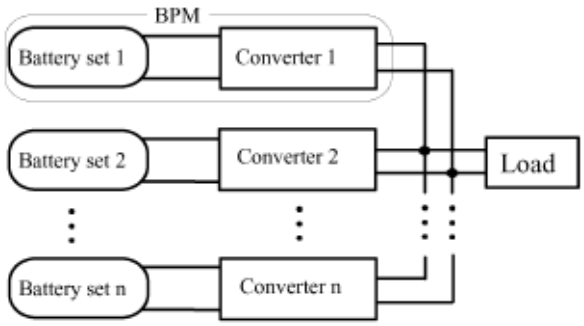

Figure 1.1: Parallel converters connected to bank of series connected battery sets [1].

A similar technique described in [21] places dc-to-dc converters on each pair of series connected cells that act as individual chargers. These converters are modified by

a programming resistor that limits the current during a charging operation to equalize all the cells while balancing. The segmented charger has been shown to properly balance a series string of battery cells. This design has shown initial promising results, however there is a significant cost associated to all the electrical components needed to use this for automotive applications.

Two other energy conversion methods, summarized in [2], are the switched transformer and the shared transformer. The switched transformer, shown in Figure 1.2, takes current from the entire pack and the transformer output is rectified through a diode. Intelligent switches are used to deliver the charge to the lower charged battery cells. This method can rapidly balance the lower cells at the cost of taking energy from the whole pack. The drawback is the low efficiency due to the switching losses and magnetics. The shared transformer has a single magnetic core with secondary taps for each cell. It also takes current from the pack into the transformer primary and induces currents in each of the secondary taps. The secondary with the least terminal voltage will have the most induced current, thus balancing the cells. This reduces the energy losses and the amount of controls needed but the complex magnetics and high parts count due to each of the secondary taps make this method rather expensive and difficult to assemble. Another example of this is shown in [22] where the balancing occurs during discharging of series-connected batteries.

A two-staged cell balancing scheme, proposed in [23], uses the same type of set up with each battery having its own converter shunted to it. However, the release of the energy from the overcharged cells is captured in a common output capacitor. This is referred to as the first stage. The second stage uses one converter that is shunted to the capacitor to send the excess energy back into the battery stack [23].

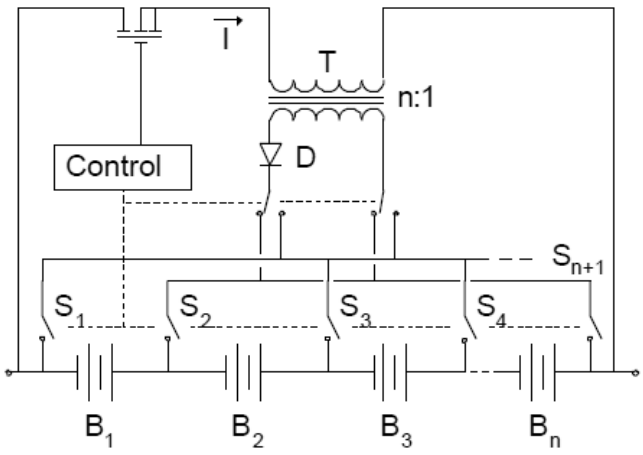

Figure 1.2: Switched transformer method used to balance series connected batteries [2].

The two-stage design removes the high voltage stress on the electrical components of the cell balancing circuits. Although there are many advantages of this design, the cost of the electrical components do not make this a practical choice for HEV and PHEV applications.

In [24], a proposed fuzzy logic controller for battery equalization is discussed. The fuzzy control set uses the cell voltages and their differences to determine the proper control for the mosfets that regulate the equalizing current in the system during either the charging or discharging state. Therefore, the mathematical model of the battery cells is not needed to describe the cell balancing system. This type of scheme was used to reduce the equalization time since it has more robustness, adaptability and better efficiency for the non-linear behavior of the cell balancing. For the design in this research, a rule-based controller will be implemented in a similar way to reduce the equalization time, however fuzzy logic will not be employed.

Another charge shuttling method that is used to balance cells in series strings is shown in Figure 1.3. A group of clocked-switched capacitors exchanges charge between adjacent cells and drives all the batteries to identical voltages without regard to component values or SoC. Through the switching, the charge is transferred from higher charged cells to lower cells. No closed loop control is needed and it can be operated during charging or operation with minimal power drain. However, the cell balancing rate occurs over a long time since there is $n-1$ capacitors, where n is the number of batteries. An extension on this design is a two-tiered capacitor design proposed in [17] and [25]. The purpose of this is to drastically reduce the cell balancing time, which is needed for automotive applications. The second tier of capacitors is aligned in parallel, one capacitor for every two first tier capacitors. This allows more charge to be transferred further along the series string in a shorter amount of time. It was shown that the balancing time can be reduced to a quarter of the time it would take its single tier counterpart. This methodology of cell balancing shows that charge shuttling can be achieved by using simple capacitors in parallel to move charge.

A variation of the charge shuttling method is to use a "flying capacitor." This reduces the amount of hardware used to implement this type of cell balancing method. By intelligently selecting which cells need to be balanced, this can dramatically reduce the time to charge balance the cells; especially if the cells are on opposite ends of the series string from each other, where the charge will not have to be shuttled through the intermediary cells to deliver the charge to the selected cell [2]. This method will be expanded upon in the research of this thesis to also "float" the capacitor between parallel strings of a battery pack. Its goal of is to reduce the electrical hardware to one capacitor per battery module for an EV or PHEV application.

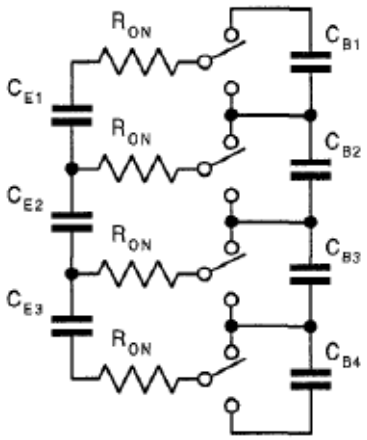

Figure 1.3: Clock-switched capacitor method used to balance series connected batteries [3].

Charge shuttling methods have a somewhat limited use for HEV applications because of the flat open circuit voltage across a broad range of SoC. HEVs are typically operated over this relatively flat range where the cell to cell voltage differences are the smallest and therefore it is rather difficult to determine the SoC of each cell in the battery pack [2]. However, this methodology is useful for EV and PHEV applications since the battery pack is routinely completely charged. The voltage difference is significantly greater between a fully charge cell and a partially charged cell.

Several proposed cell balancing methods have been discussed to prevent voltage variations within the individual cells of a battery pack and extend the life expectancy of the system. All of the active cell balancing methods use some sort of charge routing or exogenous storage device (typically a capacitor, inductor, or a combination of both) to shuttle energy between cells or groups of cells [26]. Most of what has appeared in literature to date is for series strings of batteries. This research will focus on

developing an inexpensive and efficient on board battery cell balancing system that can be used for parallel configured battery packs that will become more prevalent in advanced automotive applications, particularly PHEVs and EVs.

1.4 Outline of Thesis

Voltage drift of battery cells in various configurations affects performance and life expectancy, especially for battery packs used in automotive applications. This is a major concern, not only for individual safety, but also for warranty considerations. Monitoring and balancing individual cells of a battery pack will lead to sustained expected performance and safe operation of the battery pack within its proper operating range, while increasing the life expectancy of the cells within the pack. This research will study different methodologies that can be used to balance cells in a battery pack during no load conditions. This is ideal for battery packs used in automotive applications since they are typically only used for a couple hours a day, leaving the battery pack to rest the remainder of the time. The resting time is directly suited for the use of a properly controlled cell balancing system.

The remainder of this thesis is organized as follows. Chapter 2 discusses typical battery pack behaviors; in particular, the common problem of SoC drift in various battery pack configurations is illustrated. Chapter 3 shows the development of the battery system simulator used for the 12V module that will be the subject of extensive simulation exercises and will be tested experimentally. Then, Chapter 4 presents the detailed results of simulation with a comparison of the different types of cell balancing methods used. Chapter 5 then shows the results of the proposed active cell balancing method on the table-top experimental battery pack. Also discussed in this chapter

is the model validation based on the results obtained. Lastly, Chapter 6 reviews the results shown in this thesis along with outlining the contributions and future work that could be expanded upon this research.

Chapter 2

BATTERY PACK CHARACTERISTICS

This chapter will cover the effects and behaviors of various battery pack configurations in simulation as well as experimentation. This chapter is broken up into three sections. The first section will review the Buckeye E-motorcycle and the experimental data collected off its battery pack. The second section will review simulation data of various battery pack configurations. The last section will summarize the characteristics observed and provide motivation for cell balancing techniques.

2.1 Buckeye E-motorcycle

A Honda Nighthawk motorcycle was donated to The Ohio State University Center for Automotive Research (CAR) for a project in which it was converted into an all electric plug-in motorcycle, called the Buckeye E-motorcycle. The original engine and transmission were removed and replaced with a 19-hp electric motor, DC/DC converter, a data acquisition system, a battery pack and a cooling fan. The battery pack consists of 22 lithium-ion battery cells purchased from Lithium Technologies. The individual battery cells are rated at 3.2V and a 20Ah capacity. These batteries are connected into a single series string to form a 72V battery pack which provides the power for the motorcycle. This project has provided valuable data and information

to The Ohio State EcoCAR team during their architecture selection and battery comparison process.

The experimental data collected on the series connected battery pack is of particular interest to this research. Although the motorcycle is fully functional, it is more difficult to observe the characteristics of a battery pack during normal charge depleting operation since all the cells are being discharged. Therefore experiments were carried out on the motorcycle by connecting the battery pack directly to the 70kW load and supply located in the Battery Aging Lab at CAR. With this, charge sustaining profiles could now be run on the battery pack to observe individual cell behaviors as well as eliminate any auxiliary loads on the system, such as the headlights, which automatically function during normal operating conditions for the motorcycle.

The experiment was conducted on the battery pack to observe the open circuit voltage (OCV) drift of the individual batteries over time. A current profile, taken off a Toyota Prius battery pack during HEV mode shown in Figure 2.1, was imposed on the battery pack. There is an imposed charge period of 40A that is held for 20 seconds at the end of the active cycle, which has been added to make this a charge-sustaining profile for this experiment. The active portion of the drive cycle is approximately 500 seconds long. There is a 30 minute waiting period immediately following the profile to allow the battery pack to rest and reach a steady state value. Once the battery pack has rested for at least 30 minutes, the voltages of the individual cells are recorded using a voltmeter. The challenge in measuring the open-circuit voltage with lithium-ion batteries is the effect of polarization [27], therefore a resting period is needed for the excitation of the chemicals within the battery cells to reach steady state. Research conducted in [27], has shown that for high SoC levels (75% and

above), the voltage increases 10mV during the first half hour following disconnection from discharge and at low SoC levels (20% and below), the voltage increase of 30mV was observed over a three hour resting period. Therefore, it was determined that a 30 minute resting period would be sufficient for this experiment. This experiment was carried out until a voltage deviation of approximately 5% from nominal starting voltage was observed.

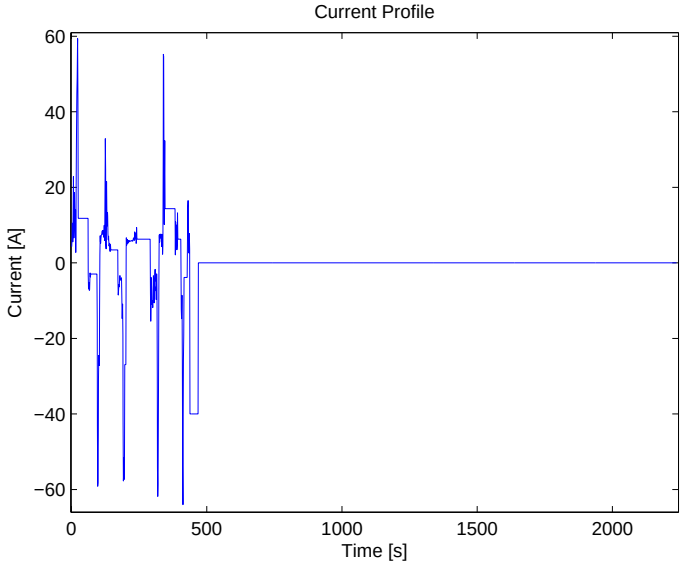

Figure 2.1: Charge-sustaining current profile from HEV drive cycle.

Since a charge sustaining current profile is used for this experiment, the total voltage of the battery pack is maintained. To validate this, the total voltage after each cycle was also recorded. It can be seen in Figure 2.2 that the overall pack voltage varies less than 0.5V over the course of 25 cycles. The total pack voltage is maintained at approximately 71V. This is critical in observing the behaviors of

the individual cells because if a cell drifts to a lower voltage, then the voltage of the remaining cells increases to maintain the overall pack voltage.

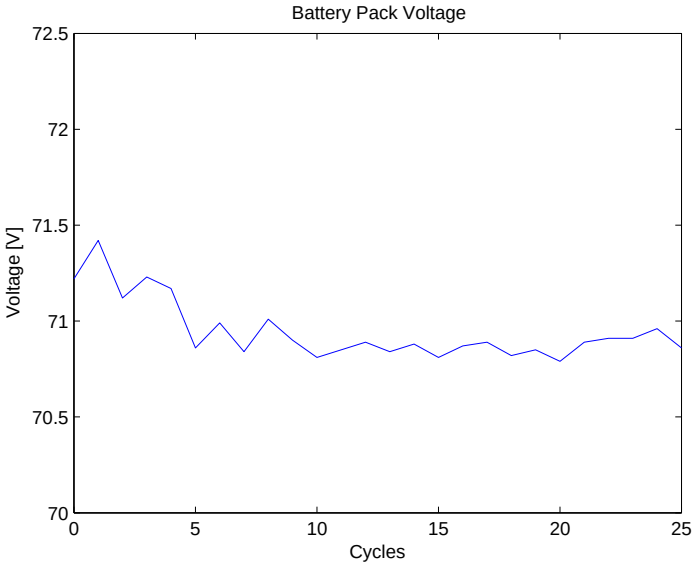

Figure 2.2: Total battery pack voltage from charge-sustaining HEV current profile.

Prior to conducting this experiment, the motorcycle was a fully functioning electric motorcycle without a BMS, driven around campus, at promotional events and sponsored tours. Proper data monitoring and logging of the individual cells was not carried out before start of this experiment and therefore the cell history, and thus the state-of-health (SoH) was not available. Therefore, the results of this experiment could potentially be skewed due the lack of an accurate charge history estimate of each of the individual cells. However, there is still valuable information to be learned even if there are aging cells in the pack since the behaviors of an aged battery pack have not been recorded.

To set up the battery pack for this experiment, it was charged up to 71V. The initial voltages of all the cells were recorded. All of the individual cell voltages were within 70mV around a nominal voltage of 3.24V. The modified, charge-sustaining HEV current profile was executed on the pack, and after every cycle, each individual cell voltage was recorded; the resulting voltages are shown in Figure 2.3.

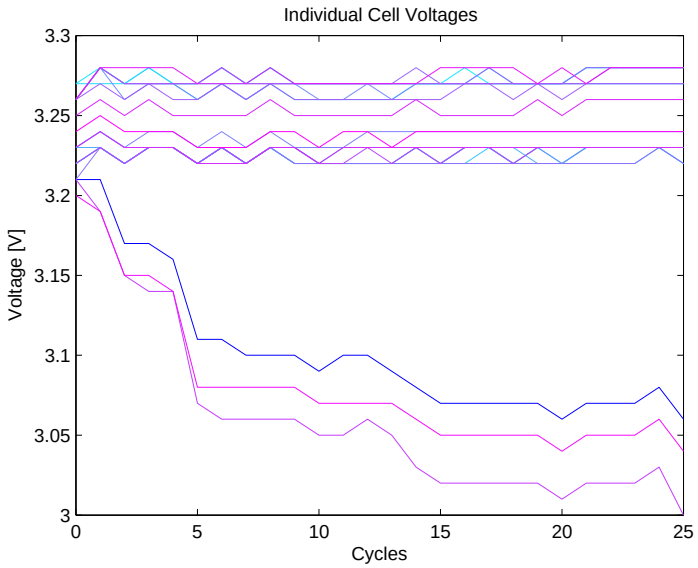

Figure 2.3: Individual battery voltage from modified charge-sustaining HEV current profile.

Examining Figure 2.3, it can be seen that there is a drift in the individual cell voltages. Specifically, there are three cells that start to drift to a lower voltage after only five cycles. Eventually, these cells drift below a voltage of 3.05V, while the remaining cells all sustain a voltage of at least 3.23V. It is important to observe the overall voltage drift of the three cells from the rest in this experiment and not necessarily important to identify the specific cells in the battery string. Since the

individual cell voltages were slightly different initially, the cell voltage deviations from their respective nominal voltages can be seen in Figure 2.4. From this figure, it can be seen that a deviation of approximately 5% occurs for the cells that are drifting to a lower voltage. The other cells have a deviation ratio that is greater than one, which shows that these cells are making up the voltage difference of the weaker cells in order to maintain the same battery pack voltage.

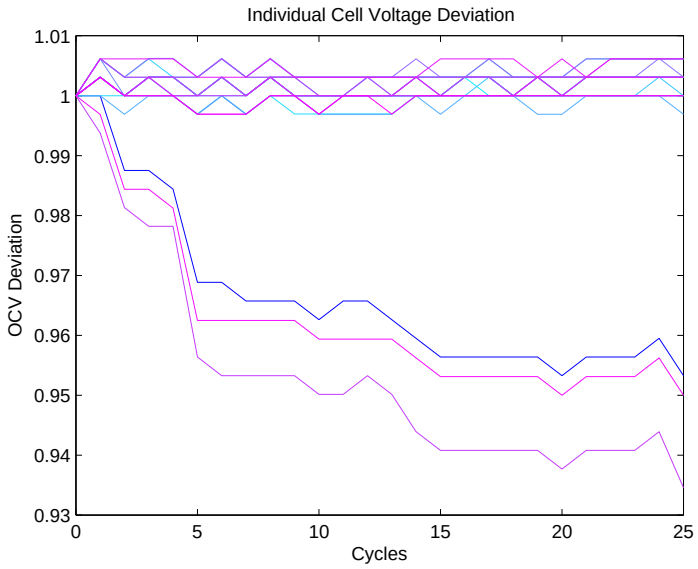

Figure 2.4: Individual voltage deviation from charge-sustaining HEV current profile.

Voltage drift is very dangerous to a battery pack because this will cause the cells that are either overvoltaged or undervoltaged to operate outside of their normal operating range if the situation is not corrected. As a result, those particular cells will undergo chemical deterioration and the expected life will be drastically reduced. This will also eventually lead to thermal runaway and potentially an explosion. Additionally, this imbalance will also cause reduced pack performance, specifically for series

string battery pack configurations. A series string of cells operates at the level of the weakest cell and if one cell is undervoltaged, the battery pack electrical potential will never be realized until that particular cell is correctly balanced.

This experiment has shown that a voltage drift can occur over a relatively short period of operation. Additionally, it has validated the necessity for a BMS. Being able to manage and properly balance the cells in this pack will extend the life and performance, as well as maintain a safe level of operation. However, it is unclear how much of an effect battery aging had on the specific cells that are tending to drift prior to this experiment.

2.2 Characteristics of a Parallel Battery Pack

In order to motivate development of cell balancing methodologies, a lumped parameter distributed battery pack model can be used to simulate the behaviors of an arbitrarily configured parallel/series battery pack. This battery pack model can resolve the dynamic effects observed for each individual cell in the pack. The model is ideal for studies in cell balancing algorithm development as well as model-based fault propagation and diagnostics [16]. The behavior of battery cells operated in a parallel configuration is of specific importance to this research. It is an ideal tool to use to analyze these effects. This simulator is explained in significant detail in the next chapter.

To develop an understanding of batteries in a parallel configuration, the model was set up to simulate a battery pack with a 3P4S (3 Parallel strings, 4 Series connected cells in each string) cell configuration, as shown in Figure 2.5. The individual cells modeled in this simulator are A123 lithium-ion cells with a nominal voltage of 3.2V

and a capacity of 2.3Ah. This results in a nominal voltage of 12.8V for the battery pack with a 7.1Ah capacity. Small battery modules such as the one that is being used for this simulation, shown schematically in Figure 2.6, can be connected to others to form a pack for automotive applications. Therefore, this is representative of a module that could be used in applications for larger battery packs consisting of smaller modules.

Figure 2.5: Table top battery pack which is represented in simulation.

This simulation was run using the same current profile that was used for the E-motorcycle experiment, which is shown in Figure 2.1. However, the imposed 40A

charge period was removed from this profile because it shows a more realistic current profile that is seen in automotive applications. This also shows more individual cell voltage deviation. To initially set up this simulation, the SoC's of each of the individual cells were arbitrarily set to 58%, thus all having the same voltage. The objective of this simulation is to observe the voltage (and therefore SoC) drift of the individual cells in the battery module over a current profile from the same starting voltage condition. The individual cells also have varied parameters, identified in [28], which shows the natural uniqueness obtained by each cell because of small manufacturing differences and unavoidable thermal gradients leading to different rates of degradation due to aging in each cell [6]. A more realistic scenario is shown how an actual battery module would behave and operate during actual operation. The internal resistance and capacity parameters, p_v, were varied using the follow equation,

$$p_v = (1 + r \times \sigma)p_b, \tag{2.1}$$

where r is a normally generated random number between 1 and -1 using the 'randn' function in Matlab, σ is the standard deviation which is set to 0.025 for this simulation, and p_b is the base parameter. Please see Appendix A for tabulated variation factors of individual cell parameters for this model.

The voltage deviation can be seen in this simulation during the active profile as well as after the load is removed from the system. Figure 2.7 shows the voltage of the individual cells over time during the experiment. The top blow-up plot of the figure shows the voltage drift once the load is removed from the battery pack. This specifically shows the final voltage drift incurred during the operation of the pack during the current cycle. After one current cycle, voltage drift can be seen within the battery pack, even though all the cells had the same initial voltage at the start

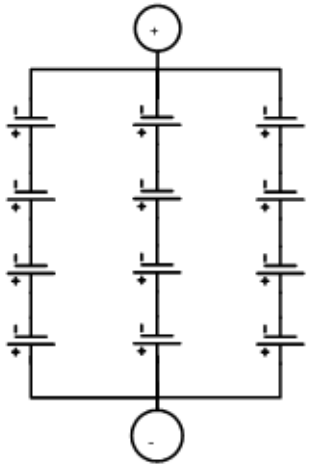

Figure 2.6: Table top battery pack schematic.

of the experiment. The lower blow-up plot shows the voltage drift that occurs during the operation of the battery pack under load conditions. The voltage separation that occurs is due to the uniqueness of each of the individual batteries and mimics the actual behavior that would be observed from an experimental setup. Even though the voltage drift is rather small in this experiment, the voltages will continue to drift further apart after several similar cycles. A severe voltage imbalance and reduced performance will result if it is not properly corrected and balanced.

Since the batteries were set with a SoC of 58%, the voltage drift is a rather difficult metric to monitor. This is because the voltage difference from one SoC percent to the next is the smallest along the OCV curve across this operating range of SoC. Therefore, monitoring the SoC of the individual cells provides a clearer comparison metric for observing cell drift. Figure 2.8 shows there is a SoC drift that is slightly over 3% after the load is removed from the battery pack. This simulation was run with a longer resting period to observe the behavior of the individual cells in this

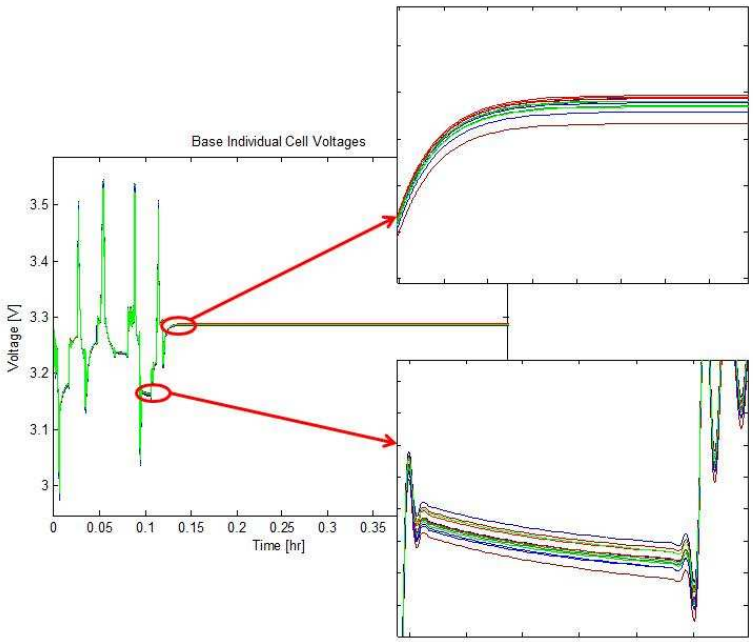

Figure 2.7: Individual cell voltage of 3P4S pack from HEV current profile.

series/parallel configuration. There is some slight convergence within the pack before the cells reach a steady state value. The convergence occurs because of the excitation of the cells within each of the strings due to their unique internal characteristics (i.e. resistances and capacitances). This SoC settling occurs as the battery pack continuously satisfies Kirchhoff's voltage law and the physical constraint where the voltages across each individual string are equal. The result of this simulation shows that imbalance occurs between the individual cells of each of the strings.

If left unbalanced, this drift will continue to get larger as more cycles similar to this one are continuously run on the pack. As stated before, this will lead to undervoltage and/or overvoltage conditions, which will lead to degradation, battery aging, and therefore a significantly reduced overall life expectancy of the battery pack. This can

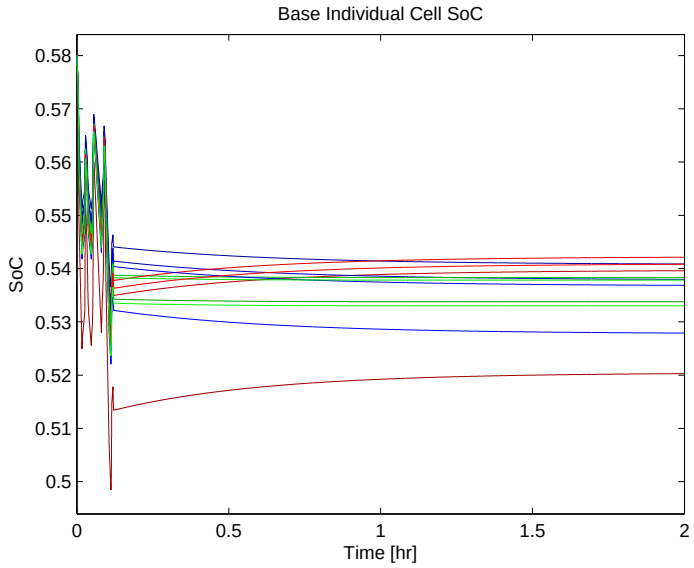

Figure 2.8: Individual cell SoC of 3P4S pack from HEV current profile.

also potentially lead to catastrophic failure of the battery pack if the imbalance is not mitigated. Additionally, this imbalance leads to reduced pack performance as the parallel strings of the battery pack will operate at the level of the weakest cell.

2.3 Summary

It is imperative that any battery cell voltage imbalances during operation be addressed. As was shown in previous sections, these imbalances can occur over a short period of time. It was demonstrated experimentally that a noticeable drift occurred in a series string after only five cycles. As mentioned before, the aging of the specific cells were unknown prior to this experiment and therefore the effect of aging on the performance of these cells is unclear. In simulation, a parallel configuration was shown to have a drift after one cycle. If not properly corrected, this drift will continue to

grow and could cause irreparable damage to the battery pack and possibly thermal runaway. An imbalance will cause a battery pack to function at a lower operating point. This results in batteries, either overvoltaged or undervoltaged, undergoing internal chemical deterioration; thus, prematurely aging the cells within the battery pack.

To minimize the effects of cell voltage drifts, imbalances must be properly mitigated. The objective of any balancing scheme is to allow the battery pack to operate at its expected performance level and extend its useful life expectancy. The following chapters will propose a passive and an active cell balancing method which has been developed to reduce the cell imbalance of a battery pack with a series/parallel configuration such as the one shown in this simulation. This type of battery configuration can be used as a module in a larger battery pack for automotive applications. Therefore, the focus of the balancing effort will be to reduce battery imbalances for a commuter PHEV. Any imbalances that accumulate over the course of driving the vehicle throughout the day, for example to and from work, will be sufficiently balanced when the battery pack is under no-load conditions, such as during work or overnight hours while the pack is resting. The objective of the on board active balancing system is to achieve proper cell balancing by the time the vehicle is put back into service. This provides a target time estimation of between 8 to 12 hours to balance the battery pack on board the vehicle.

Chapter 3

BATTERY SYSTEM MODEL: ANALYSIS AND CELL BALANCING CONTROL

This chapter describes the development of the battery system model simulator. The model not only includes the individual cells of the battery pack, but also two different types of cell balancing methods developed for research in this thesis. The next section gives an overview of the entire system model. Next, the identification of a lithium-ion battery cell is discussed. The development of the battery pack model is then reviewed. The next two sections will examine the active and passive cell balancing design implementations, respectively. Then the comparison between the two algorithms using constant parameters and varying parameters is discussed. Lastly, the complete battery system model simulation steps are summarized.

3.1 Battery System Model Overview

A dynamic battery system model was developed to simulate the electrical dynamics of all the cells and cell balancing components of an arbitrary parallel/series battery pack configuration, as shown in Figure 3.1. The simulator is based on the development of an analytical solution for the response of a single cell in the pack.

The elemental solutions can then be used to solve for the dynamic behaviors of the distributed pack model and cell balancing circuit.

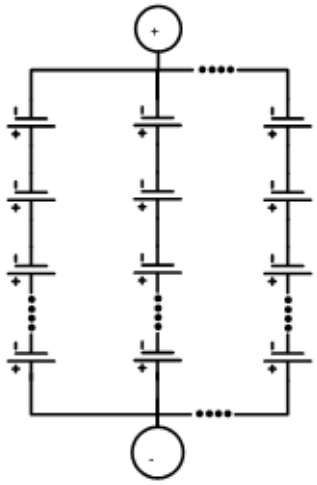

Figure 3.1: General battery pack topology.

The battery system model was designed using analytical solutions because this leads to a computationally efficient tool which is appropriate for large scale battery pack applications. The battery pack configurations used in this simulator are those that are typical for automotive applications. This simulator can simultaneously compute the results of configurations with a passive or active cell balancing system, or none at all, using typical automotive current profiles for battery packs made of cells with a random distribution of parameters. This allows for a simulation comparison analysis on various battery pack configurations. This will also lead to an experimental comparison for model validation.

3.2 Single Lithium-Ion Battery Cell Model

A simplified low-order, model-based approach is advantageous for control algorithm implementation. Therefore, an equivalent circuit model was chosen as the model for each single cell. Other modeling approaches, such as electrochemical battery modeling (see [29, 30]) often involve complex partial differential equations to describe the highly dynamic response of the battery as well as ion diffusion and other electrochemical properties. An analytical solution to the dynamic battery model is also necessary because traditional numerical solutions (such as using an ODE solver) can be computationally intensive, thereby prohibiting large scale battery pack simulation (especially packs with multiple parallel strings) due to the need to evaluate many single cell battery models in one simulation time step [16].

Thus, a low-order equivalent circuit model has been chosen (2^{nd} order). The model structure of the equivalent circuit battery model consists of an internal resistance, two parallel RC circuits, and an ideal voltage whose output is referred to as the open circuit voltage (OCV). Figure 3.2 shows the basic equivalent circuit model employed.

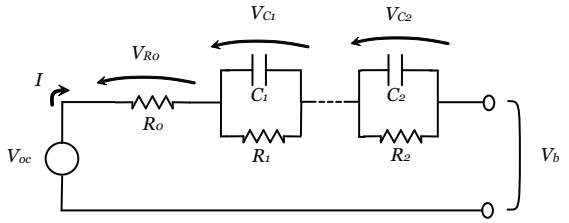

Figure 3.2: Equivalent circuit model for a single battery cell.

The voltage $V(t)$ across the battery is given by

$$V(t) = E_0(t) - R_0 I(t) - V_{c1}(t) - V_{c2}(t), \tag{3.1}$$

where $E_0(t)$ is the ideal voltage source (which essentially models the OCV), R_0 is the internal resistance, $I(t)$ is the current input (as seen by the battery), and $V_{ci}(t)$ is the voltage across the independent first-order RC circuit combinations, which can be described by an ordinary differential equation obtained by using Kirchoff's current law and the definition of an ideal capacitor,

$$\frac{dV_c}{dt} = -\frac{1}{R_C} V_c(t) + \frac{1}{C} I(t). \tag{3.2}$$

The methodology for identifying the parameters and the closed-form solution are reviewed in the next two subsections.

3.2.1 Parameter Identification

Research has been done at The Ohio State University's Center for Automotive Research Battery Aging Lab identifying lithium-ion battery parameters by several graduate students. An A123 lithium-ion cell (2.3Ah, 3.2V nominal) was used as a the prototype for identifying all the base battery parameters. A three step process defined by [28, 16] was used to identify all the parameters:

1. Gather experimental data
2. Identify OCV curves
3. Identify SoC-dependent coefficients for equivalent circuit

The parameters of the equivalent circuit are identified as piecewise linear continuous functions (linear splines). It is significantly cheaper in terms of computational efficiency to use linear splines rather than using a higher order polynomial to represent the dynamic effects across the high and low values of the SoC range.

It is easier to visualize Equation 3.2 more generically in terms of a *time constant* and an *input coefficient*. Therefore, it can be rewritten as

$$\dot{V_i} = A_i V_i + A_i B_i I. \tag{3.3}$$

where A_i is the inverse of the *time constant* of the dynamic system, V_i and B_i are the steady state scaling factors for the *input coefficient* [28]. A_i and B_i are functions of the direction of the current and SoC since the values for the resistance and capacitance are functions of these variables. Batteries typically behave differently depending on whether they are being charged or discharged. The parameters are separately specified for each dependence, the first being with respect to the direction of the current. The parameters are defined as follows:

$$A_i = \begin{cases} A_i^+(SoC) & \text{if charging} \\ A_i^-(SoC) & \text{if discharging} \end{cases} \tag{3.4}$$

$$B_i = \begin{cases} B_i^+(SoC) & \text{if charging} \\ B_i^-(SoC) & \text{if discharging} \end{cases} \tag{3.5}$$

where $A_i^{\pm}(SoC)$, and $B_i^{\pm}(SoC)$ become functions of SoC only. The OCV curve is then defined as a continuously *increasing* function dependent upon the SoC. A linear spline is also an ideal representation of the OCV curve because it is very difficult to constrain a polynomial to be an increasing function.

The first step in identifying these parameters is to gather experimental data. The battery aging lab is equipped with several battery cylinders and environment control chambers which are used to perform experimental tests. Several capacity tests are initially run to determine the actual battery capacity. A current step profile is then executed, which takes the battery through a range of SoCs in order to adequately

model the usable range of the battery cell. The resulting current, voltage, and temperature measurements are recorded and then used as inputs into the identification algorithm.

The identification algorithm uses a genetic algorithm (GA) optimization methodology developed at The Center for Automotive Research. The GA program written in FORTRAN is run on a parallel computing cluster using the experimental data obtained as bounds to obtain an OCV curve from the experimental cell to reduce the computation time. The SoC-dependent coefficients are then identified using a GA along with the identified OCV curve. A constant model is first identified and then the linear parameter varying (LPV) model is identified. Along with the well defined bounds of the constant model identification, the constant model parameters found are used as the initial starting points for the search to find the linear splines that represent the coefficients of the LPV model. These linear spline coefficients are then put into the equivalent circuit model as described by Equation 3.1. Refer to [28] for a detailed description and experimental results of this identification procedure. Additional applications of automotive system modeling using linear parameter varying models can be found in [31].

3.2.2 Battery Cell Model Structure

In order to obtain a closed-form solution to the differential equation for a battery simulation, and ultimately to specify $V(t)$, it is assumed that $E_0(t)$ and $I(t)$ are constant across a time step. This is a reasonable assumption because the current profile to be used in simulation will be sampled at very small intervals (for example,

0.01 or 0.1 seconds). Thus the current input will be considered a step function (defined as having a value of i_b across the time interval of interest).

The voltage across the capacitor is given by

$$\dot{v}(t) = -\beta v(t) + \gamma i_b(t) \tag{3.6}$$

where $\beta = \frac{1}{RC}$ and $\gamma = \frac{1}{C}$.

To find a closed from solution, rearrange and multiply both sides by $e^{\beta t}$ to get

$$e^{\beta t}(\dot{v}(t) + \beta v(t)) = e^{\beta t}\gamma i_b(t). \tag{3.7}$$

Recognizing the fact that

$$e^{\beta t}\gamma i_b(t) = \frac{d}{dt}(e^{\beta t}v(t)), \tag{3.8}$$

it is possible to write

$$\frac{d}{dt}(e^{\beta t}v(t)) = \beta e^{\beta t}v(t) + e^{\alpha t}\dot{v}(t). \tag{3.9}$$

Then integrating from t_0 to t results in

$$e^{\beta t}v(t) - e^{\beta t_0}v(t_0) = \int_{t_0}^{t} e^{\beta \tau}\gamma i_b(\tau)d\tau. \tag{3.10}$$

Since $i(t)$ is specified as constant across an interval, the expression can be rearranged to give

$$v(t) = e^{-\beta(t-t_0)}v(t_0) + e^{-\beta t}\int_{t_0}^{t} e^{\beta \tau}\gamma i(\tau)d\tau. \tag{3.11}$$

Evaluating the integral term on the right-hand side, it is found that

$$e^{-\beta t}\int_{t_0}^{t} e^{\beta \tau}\gamma i(\tau)d\tau = \frac{\gamma i_b(t)}{\beta}(1 - e^{-\beta(t-t_0)}) \tag{3.12}$$

Thus, the expression for a constant forcing current across a specified time interval is given as

$$v_c(t) = e^{-\beta(t-t_0)}v_c(t_0) + \frac{\gamma i_b(t)}{\beta}(1 - e^{-\beta(t-t_0)}), \tag{3.13}$$

for $t > t_0$. In fact, if the interval is constant (that is, if $T = t - t_0$), then

$$V_c(t) = e^{-\beta T} V_c(t_0) + \frac{\gamma i_b(t)}{\beta}(1 - e^{-\beta T}). \tag{3.14}$$

The V_c expression derived above can be used in both dynamic expressions in Equation (3.1) since the second dynamic (V_{c2}) is simply a second cascaded RC circuit in the model. Refer to [16] for a more detailed description of this derivation to be used for simulation. By using identified parameters from the experimental data with this single cell battery model, a full battery pack model can be simulated.

3.3 Battery Pack Model

Using the single cell equivalent circuit model derived in the previous section, a pack model can be constructed with various cells connected in series and in parallel. One of the major challenges is designing a battery pack model with parallel strings to be used in simulation is defining the current splits during simulation runtime. Thus, the model representation must allow for current splits between the strings to be calculated during the runtime of the simulation [16].

3.3.1 Battery Pack Model Structure

The notation of the battery pack uses a matrix-like topology for clarification, where the columns of the matrix represent the batteries that are connected in series and the rows in the matrix represents the number of cells in each string. Therefore, a subscripting notation is used. The ideal voltages for each of the batteries is represented as $E_{i,j}$, where i is the notation for the battery in the i^{th} row, and j is the notation for the battery in the j^{th} column (or string) of the battery pack. Similarly, $R_{0[i,j]}$ represents the internal resistance of the $(ij)^{\text{th}}$ battery, $R_{k[i,j]}$ represents the k^{th}

resistor of the $(ij)^{\text{th}}$ battery in the pack model, and $C_{k[i,j]}$ represents the k^{th} capacitor of the $(ij)^{\text{th}}$ battery cell model in a pack. The current is the input (as seen by each battery) denoted as α_j, which is the current through the j^{th} string (or battery column) of the pack. Therefore, $V_j(t)$ represents the string voltages for each of the strings in the battery pack and $V_{ck[i,j]}$ represents the voltage across the k^{th} capacitor in the model.

Using this subscripting notation to identify the elements of the model, the equations used to derive the model becomes more clear. Since the battery strings are connected in parallel,

$$V_1(t) = V_2(t) = \ldots = V_n(t), \tag{3.15}$$

where n is the number of parallel strings in the pack. To include the current input (forcing function as seen by the parallel combination of batteries), it is noted that a simple application of Kirchhoff's current law renders

$$I = \alpha_1 + \alpha_2 + \ldots + \alpha_n, \tag{3.16}$$

which is constant across a simulation time step.

By examining the definition of each battery model in parallel, it is now clear that the entire system can be represented as a solution of linear equations. To simplify notation, we will define

$$\Phi_j = \sum_{i=1}^{m}(-R_{0[i,j]} + R_{1[i,j]}(1 - e^{-\beta_{1[i,j]}t}) + R_{2[i,j]}(1 - e^{-\beta_{2[i,j]}t})) \tag{3.17}$$

and

$$\Gamma_j = \sum_{i=1}^{m}(E_{i,j} + \bar{V}_{c1[i,j]}(1 - e^{-\beta_{1[i,j]t}}) + \bar{V}_{c2[i,j]}(1 - e^{-\beta_{2[i,j]t}})), \tag{3.18}$$

where m is the number of batteries in each string. From Equations (3.16), (3.17), and (3.18), a generalized system of linear equations can be constructed to represent

the current split between the parallel string connections:

$$\begin{bmatrix} \alpha_1 \\ \alpha_2 \\ \alpha_3 \\ \vdots \\ \vdots \\ \alpha_n \end{bmatrix} = \begin{bmatrix} \Phi_1 & -\Phi_2 & 0 & \cdots & \cdots & 0 \\ 0 & \Phi_2 & -\Phi_3 & 0 & \cdots & 0 \\ 0 & 0 & \Phi_3 & -\Phi_4 & \cdots & 0 \\ \vdots & \vdots & \vdots & \ddots & \ddots & \vdots \\ \vdots & \vdots & \vdots & \vdots & \Phi_{n-1} & -\Phi_n \\ 1 & 1 & \cdots & \cdots & 1 & 1 \end{bmatrix}^{-1} \begin{bmatrix} \Gamma_2 - \Gamma_1 \\ \Gamma_3 - \Gamma_2 \\ \vdots \\ \vdots \\ \Gamma_n - \Gamma_{n-1} \\ I \end{bmatrix}, \tag{3.19}$$

where n is the number of parallel strings in the battery pack, α_j is the current through each string, and I is the total current seen by the entire pack.

By adding more strings in parallel to the battery pack, the size of the Φ matrix (while maintaining it as a square matrix) will increase. For an arbitrary number of parallel strings, the Φ matrix (that is, the matrix containing terms represented by Φ) will always take the structure of a bidiagonal matrix with a row of 1's representing the equation for the current. This is due to the fact that each battery string voltage is set equal to the next string in the pack. A simple example of this is two batteries connected in parallel to form a 2P1S (2 Parallel, 1 Series) configured battery pack. The system of linear equations to represent the current split between the two batteries in a parallel pack connection is given by

$$\begin{bmatrix} \alpha_1 \\ \alpha_2 \end{bmatrix} = \begin{bmatrix} \Phi_1 & -\Phi_2 \\ 1 & 1 \end{bmatrix}^{-1} \begin{bmatrix} \Gamma_2 - \Gamma_1 \\ I \end{bmatrix}. \tag{3.20}$$

Refer to [16] for a more detailed explanation of the derivation used in simulation as well as the experimental results that validate this battery pack model. With this battery pack model representation, an active cell balancing system can be now be modeled and implemented.

3.4 Active Cell Balancing Control

As described in [3], a switched capacitor scheme shuttling charge to adjacent cells was shown to increase the energy efficiency along a series string of connected battery cells. [2] shows an extension of this by using a "flying capacitor" which moves along the series string by intelligently closing switches around the desired cell to achieve balancing. The flying capacitor only uses one capacitor for the entire series string whereas the switched capacitor method uses $n-1$ capacitors for a string of n batteries. The flying capacitor used in [2] increases the complexity of the control but significantly reduces the amount of electrical components needed, since it can shuttle charge to opposite ends of the battery string. Therefore, the component and installation costs are reduced.

The active cell balancing approach designed for the simulator of this work uses a "floating capacitor". The need for increased battery pack capacity, for a given voltage, requires more battery strings in parallel. The proposed "floating capacitor" design expands on these previous designs by using the capacitor across multiple series strings, thus eliminating the need for a different balancing circuit for every string. This method proposes only one capacitor for a battery module, which consists of both series and parallel strings. An example of this cell balancing circuit structure on a 3P4S battery pack can be seen in Figure 3.3. These modules can then be connected together forming an entire pack for use in a range of hybrid vehicle applications. The motivation behind this design was to reduce the circuit complexity as well as the packaging and installation costs. This research focuses on the feasibility and development of this active cell balancing system on a module and therefore assembling an

entire pack is outside the scope of this thesis. Thermal effects are also not considered within the realm of this thesis, but should be accounted for in future work.

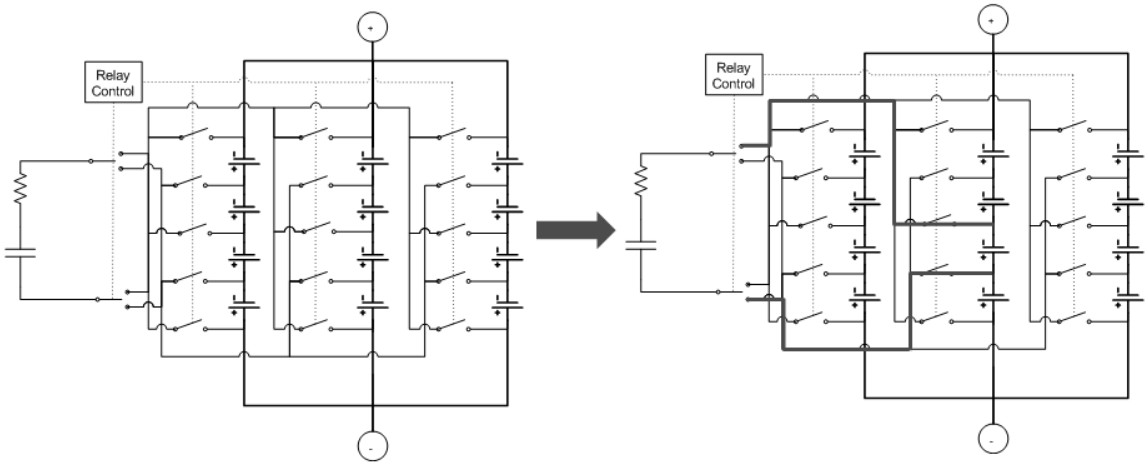

Figure 3.3: Active balancing control circuit.

3.4.1 ACB Cell Balancing Circuit Structure

An equivalent circuit model has been selected to model the cell equalization circuit, which can been seen in Figure 3.4. With the assumption that the system is under no load, the cell balancing circuit model consists of a resistor, R, and a capacitor, C, connected in series with the battery in the module that has been intelligently selected to be balanced. A current is induced by the voltage difference between the battery and the capacitor. The direction of the current will depend on whether or not the capacitor voltage is greater than (charging) or less than (discharging) the battery to which it is connected. The battery voltage, V_b, was derived in the previous section. The capacitor will be used to transfer charge from high voltage cells to lower voltage

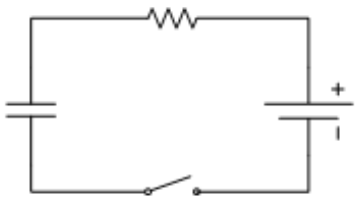

Figure 3.4: RC circuit for active balancing of a single battery cell.

cells. The resistor in the circuit is used to regulate the current between the battery and the capacitor. The equation for the circuit shown in Figure 3.4 can be expressed as

$$V_b(t) = RI_c(t) + V_c(t), \tag{3.21}$$

where V_b is the battery voltage at time step t and V_c is the capacitor voltage at time step t. The final value of the capacitor voltage after the current source has stopped charging the capacitor depends on two factors: (1) the initial value of the capacitor voltage and (2) the history of the capacitor current. An analytical expression for the current must be obtained before the capacitor voltage can be solved. The current, $I_c(t)$, can be expressed as either positive or negative, which indicates whether the battery is discharging or charging, respectively. Substituting the equation for the voltage across a capacitor into the previous equation results in

$$V_b(t) = RI_c(t) + \frac{1}{C}\int_{t_{0^+}}^{t} I_c(\tau)d\tau + V_c(t_{0^-}), \tag{3.22}$$

where the integration of the current is over the present time step and $V_c(t_{0^-})$ is the voltage of the capacitor at the end of the previous time step. The Laplace transform can be use to derive the induced current expression because the battery voltage is assumed to be constant across a time step. First, the expression is multiplied by C

on both sides

$$V_b(t)C = RCI_c(t) + \int_{t_{0+}}^{t} I_c(\tau)d\tau + V_c(t_{0-})C. \tag{3.23}$$

The Laplace transform is now applied, leaving

$$\frac{V_b(s)C}{s} = RCI_c(s) + \frac{1}{s}I_c(s) + \frac{V_c(s_{0-})C}{s} \tag{3.24}$$

and both sides are multiplied by s to give

$$V_b(s)C = RCsI_c(s) + I_c(s) + V_c(s_{0-})C. \tag{3.25}$$

Simplifying the expression and factoring out a C and $I_c(s)$ reveals

$$C\big(V_b(s) - V_c(s_{0-})\big) = I_c(s)(1 + RCs). \tag{3.26}$$

Solving for the current gives

$$I_c(s) = \frac{C\big(V_b(s) - V_c(s_{0-})\big)}{1 + RCs}. \tag{3.27}$$

An R factor is introduced on the right-hand side of the equation to simplify the inverse Laplace transform

$$I_c(s) = \frac{RC}{1 + RCs}\frac{\big(V_b(s) - V_c(s_{0-})\big)}{R}. \tag{3.28}$$

This can now be simplified and the current expression becomes

$$I_c(s) = \frac{1}{s + \frac{1}{RC}}\frac{\big(V_b(s) - V_c(s_{0-})\big)}{R}. \tag{3.29}$$

This can now be inverse transformed into

$$i_c(t) = \frac{\big(V_b(t) - V_c(t_{0-})\big)}{R}e^{\frac{-t}{RC}}. \tag{3.30}$$

The analytical solution for the voltage across the capacitor can now be solved for by substituting the induced current solution into

$$V_c(t) = \frac{1}{C}\int_{t_0^+}^{t} i_c(\tau)d\tau + V_c(t_{0^-}), \tag{3.31}$$

where the current is integrated across the present time step and $V_c(t_{0^-})$ is the initial voltage that was solved for at the end of the previous time step.

Other battery pack behaviors arise when adding additional parallel strings. Referring back to Kirchhoff's voltage law for parallel strings in Equation (3.15), the string voltages are equal. The batteries within the strings have slightly different internal characteristics, most notably internal resistances. This results in induced mesh currents between the parallel strings, which the battery pack model incorporates and solves for when determining the current split in Equation (3.19). These mesh currents also occur during operation as well as when the battery pack is under no-load conditions. The induced current in the ACB circuit is also treated as a mesh current for the particular battery cell to which it is connected at that specific time interval. Therefore, this current must also be accounted for when calculating the voltage of the battery that is connected to the ACB circuit.

The current in the cell balancing circuit, i_c, was found in Equation (3.30). Therefore, when determining the voltage of the battery connected to the balancing circuit, the induced current from the balancing circuit and the mesh current, i_m, induced from the voltage imbalance of the parallel battery strings are additive thus resulting in the observed battery current, i_b, given as

$$i_b(t) = i_c(t) + i_m(t). \tag{3.32}$$

3.4.2 ACB Control Strategy

The objective of the active cell balancing circuit is to transfer energy from battery cells with a higher charge to cell with a lower charge and effectively balance the entire pack when in a no-load condition. It accomplishes this by measuring the voltages of all the cells to determine which have a higher SoC and which have a lower SoC. A rule based control strategy is used which intelligently selects the highest charged cell and the lowest charged cell to balance, regardless of the location in the battery pack.

At every time interval, each of the battery voltages are recorded. The highest voltage and the lowest voltage are selected for balancing. The switching occurs continuously between these two cells until either the selected large cell no longer has the largest voltage or the small cell no longer has the lowest voltage. At that point a new high or low (or both) cell are determined for balancing. The balancing continues until the voltage imbalance across all the cells in the pack is small enough or until there is a load applied to the battery pack itself.

A rule based approach was deemed appropriate because a membership or cost function does not need to be defined. At each time interval, there is always a battery cell with the maximum voltage and there is always a cell with the minimum voltage. Thus, a penalty does not need to be applied to selecting any other cell for balancing, since only the minimum and maximum cells are selected. Therefore, a fuzzy logic approach is not needed. The rule-base is ordered as follows:

1. Check for a no-load input current.

2. Set switching frequency to selected RC time constant.

3. Determine which two cells have the maximum voltage deviation *between each other*; these are selected for balancing.

4. Cell balancing occurs if the SoC deviation of the selected battery cells is greater than 1.0%, or $SoC_{Vmax} - SoC_{Vmin} > 1.0\%$.

5. Start switching from the cell with the maximum voltage if its voltage is larger than the initial voltage of the capacitor, $V_{max} > V_c$, otherwise start switching from the selected cell with the minimum voltage.

6. Stop balancing if safety bounds of the system are violated during operation.

Additional checks are also performed to guarantee that each cell voltage of the battery pack is operated within the safety region during the cell balancing operation. The capacitor and the resistor in the cell balancing circuit are also monitored to make sure neither function outside of their respected operating ranges.

3.5 Passive Cell Balancing Control

The passive cell balancing (PCB) system used with this simulator is primarily used as a tool for comparison against the active cell balancing design. The PCB approach designed for this simulator uses a shunt resistor across every battery in the pack, as shown in Figure 3.5. The shunt resistors are intended to dissipate excess charge as heat from the individual cells that are determined to have a higher voltage than others in the pack. Switches are controlled to regulate the dissipative action of the resistive circuit. This type of cell balancing system was derived from the I+ME BMS that was purchased for the electric motorcycle. As mentioned in Chapter 2, the motorcycle has a battery pack that consists of 22 series connected lithium-ion

batteries, which was designed and built by students at The Ohio State University Center for Automotive Research. The intended design for this BMS was to be used on a battery pack with a one series string orientation. This cell balancing concept has been expanded upon in this proposed design to encompass battery packs with multiple parallel strings.

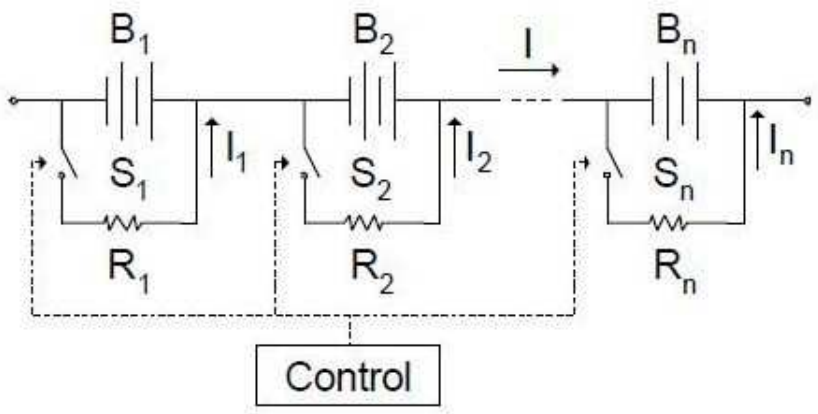

Figure 3.5: Charge shunting circuit for passive balancing of a string battery cells [2].

The goal of the passive balancing system is to bring the cell voltage differences to a value given by the parameter $VoltSet$, which is the average difference of the individual cell voltages plus the minimum cell voltage once the battery pack is not in operation mode. After the battery pack is brought to a no-load input current condition, a timer counts to 30 minutes. When the timer expires, the $VoltSet$ parameter is calculated. The resting duration was deemed sufficient enough for this application to allow the individual batteries to relax. The timer is reset and the switches for the balancing circuit are opened, thus stopping the balancing, when a load is applied to the battery pack. The voltage balancing point is recalculated in the same fashion once the 30

minute timer again expires when the battery pack has been under no load current. The higher voltage cells will be simultaneously discharged until the target is reached ($AvgDelta + CellMin$). This is only valid for cells that have a voltage that is higher than this parameter; cells with a voltage less than this are never discharged by the balancing system. Therefore, balancing of every cell cannot be reached under all circumstances. Figure 3.6 shows an example of battery cell voltages in a pack prior to balancing with the voltage set point. All the cells with a voltage above the shown set point will be discharged until their respective voltages reach this set point value.

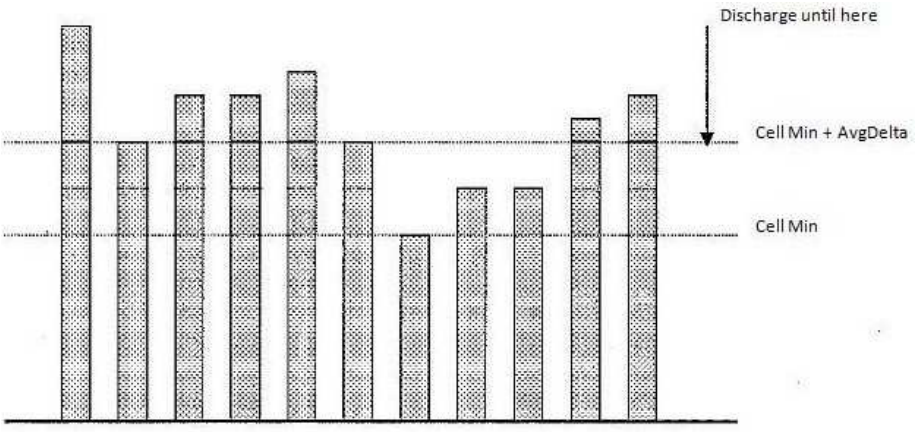

Figure 3.6: Voltage bar chart for passive balancing [4].

The electrical components required for this type of balancing involves one switch and one resistor for every cell in the battery pack. The resistors are sized to 50Ω to set the discharge current used by the balancing circuit to approximately 65mA for each of the cells. This is done to reduce the amount of heat being dissipated at one time.

As with the implementation of the active balancing system, similar behaviors arise due to the parallel configurations of the battery pack. Each of the shunt resistors also create a parallel circuit when connected to its respective battery. Therefore, an induced current from the balancing circuit must again be accounted for when determining the voltage of the particular cells that are affected by the balancing at a specific time interval. These induced currents are treated as mesh currents which are additive to the currents that exist in the voltage imbalance with the parallel configuration of the battery pack.

3.6 Battery Model Parameters Comparison

As described in Section 3.2.1, the battery identification is completed by first using constant parameters. These constant parameters are then used as a starting point for the identification process for the linear splines used for the LPV model. Both the constant and LPV parameters were identified and verified with experimental data in [28]. The constant parameters are useful as a quick estimation for modeling the characteristics of a battery. These are typically employed when developing a larger scale simulator to simplify the debugging process and reduce simulation time but still provide a relatively accurate battery estimation. Once simulator development is sufficient enough that the parameters pose no errors, then LPV parameters can be applied. LPV parameters provide a more precise estimation of individual battery cell behavior over various temperature and current profiles. The parameters are scheduled based on input current, temperature and SoC. The input current is specified as a parameter for the model because there are two battery operating modes, charging and discharging. There are two different linear splines that are identified for each

of the operating modes. These are identified separately due to different efficiencies observed when operating in the different modes. Therefore, using LPV parameters provides a more accurate model in which the behavior of the individual cells can be affected by several variables (i.e. input current, temperature, SoC).

3.7 Simulation Strategy for the Complete Battery System Model

With the modular design of the simulator, this battery system model can be simulated across any array of battery module configurations by selecting how many batteries there will be in series as well as how many parallel strings. In order to simulate the pack model defined in the previous sections, a couple of assumptions must be made:

1. The current input to the system and the induced current of the cell balancing circuit is constant over a simulation time interval.

2. The SoC (and therefore the E_0) of each battery does not change significantly over a simulation time interval.

The first assumption is made in order to use the battery model defined in the previous sections. The second assumption can be made because it is assumed that the time interval is small enough so that the there are no large SoC or E_0 changes from one simulation instance to the next (sampling on the order of 10Hz). Both of these assumptions are reasonable for the this application [16].

The simulation of the battery pack algorithm with the cell balancing circuit is carried out as follows:

1. Define battery characteristics for each individual cell.

2. Define cell balancing circuit parameters

3. Set up initial conditions for each battery (i.e. set SoC/OCV equal to represent a pack at equilibrium and battery capacitor voltages ($V_{ck[i,j]}$) set to 0V to simulate a completely relaxed battery.)

4. Evaluate first simulation time step using first value of input current profile with initial battery parameters and SoC.

5. Begin simulating current profile.

6. Calculate battery parameters and OCV[1] as a function of current battery SoC, current input, and individual battery characteristics.

7. Construct Φ and Γ matrices using perturbed or base battery parameters.

8. Use the Φ and Γ matrices to solve for the current split of the next simulation time step.

9. Locate the battery cells in the pack with the minimum and maximum voltages for balancing.

10. Evaluate balancing circuit voltage, V_c, and current, i_c, if the battery pack is under no-load current conditions.

11. Evaluate the SoC, $V_{c1[i,j]}$, and $V_{c2[i,j]}$ for each battery in the pack, including the effects of the balancing circuit on the battery to which it is connected.

[1]The OCV can be calculated based on the previous step's SoC because it is assumed that the battery SoC does not change drastically over a simulation time step

3.8 Summary

The development of the battery system simulator has been a culmination of various research projects that have been completed at The Ohio State University Center for Automotive Research. The 2nd-order equivalent linear parameter varying single battery model was first explained. An entire battery model with an arbitrary series/parallel configuration with LPV parameters for the individual batteries was discussed. Two cell balancing methodologies were then derived as an application for the battery pack. Lastly, the overall battery system model simulation strategy was reviewed. This system model will provide simulation data to support the feasibility of such a cell balancing network in hardware implementation.

The next chapter will describe the simulation development and evolution of the simulator with data to support the relevant findings. An active cell balancing component sizing comparison will be completed as well as a comparison of either balancing system to the base pack with no balancing. Additional unique cases will also be simulated and analyzed based on drive test data collected at CAR.

Chapter 4

SIMULATION RESULTS FOR THE COMPLETE BATTERY SYSTEM MODEL

This chapter provides simulation results of the entire battery system model throughout the development process. The next section will focus on the single cell ACB circuit with constant battery parameters. Next, before moving to a full pack model, simulation of the model with charge shuttling between two cells connected in series is discussed along with an energy efficiency and balancing rate comparison according to the appropriate sizing of the ACB components. Then, the simulation results of the complete ACB simulator with an arbitrarily selected series/parallel configuration will be reviewed. The next section will analyze the complete PCB simulator. Lastly, a comparison between the various cell balancing techniques and the non-balanced battery pack will be conducted using the model with LPV characteristics included.

4.1 Single Cell ACB Circuit

The simulator was developed and built in an m-file with analytical solutions used to represent the system equations for the second-order battery cell model as well as the capacitor voltage and the induced current of the cell balancing circuit. The motivation behind creating a simulator based on the analytical solutions rather than a Simulink

model is the simulation run time is considerably less because the s-functions and look-up tables that would be needed to be in embedded in the Simulink model are more computationally intense as explained earlier. The first step was to model the behavior of the ACB with an RC circuit connected to a single battery. The second-order battery model used for this simulation is a constant parameter model representing a 2.3Ah, 3.2V, A123 lithium-ion battery [28]. Constant parameters were used to reduce the amount of errors for debugging purposes when building the simulator. Additionally, having constant parameters reduces the simulation run time.

It was determined that a time step of 0.1 seconds is sufficient enough to model and simulate the system characteristics without losing any resolution since the battery is a naturally slow system. Based on the assumptions made in Section 3.7, the voltage of the battery and the capacitor as well as the current induced between them is assumed to be constant across this time step. Another assumption, based on the cell balancing, was that this action only occurs under no-load conditions of the battery pack. With this assumption, when the balancing circuit is connected to one of the batteries, it creates a RC series connection and a current is induced between the two energy storage components described in Equation 3.30. When the balancing circuit is connected, the voltages of the battery and the capacitor will attempt to balance over time, thus either adding or removing charge from the battery.

An example of this was simulated with a battery initially set to 60% SoC, which correlates to approximately 3.296V, and a balancing circuit consisting of a 100mΩ resistor and a 30F capacitor with an initial voltage of 3.29V. Figures 4.1 and 4.2 show the voltage and current behaviors of the RC circuit when it is connected to the battery. The simulation time was set for 10 seconds. The ACB circuit was closed at 1

second and then opened at 6 seconds. The initial drop in voltage seen by the battery is due to the dynamics and internal resistance of the battery. Once the ACB circuit is disconnected from the battery, the capacitor voltage stays the same, the battery relaxes, and its voltage settles to a steady state value. Figure 4.2 also shows that the current is greatest when the switch is first closed and gets exponentially smaller as the voltage difference becomes smaller. The voltage drop is expected to be the greatest at this point because the current is also the largest. Figure 4.1 also shows that the final voltage of the capacitor voltage has increased and the battery voltage has slightly decreased, thus resulting in an energy transfer from the battery to the capacitor.

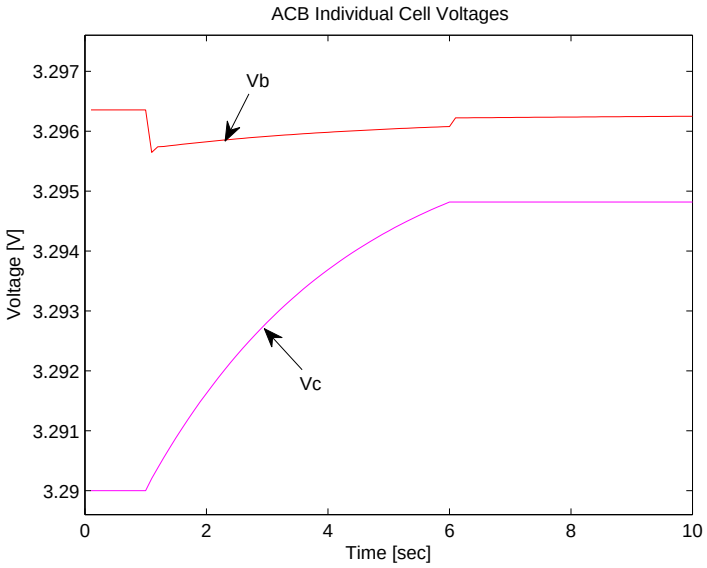

Figure 4.1: Voltage behavior of circuit elements when ACB is connected to a single cell.

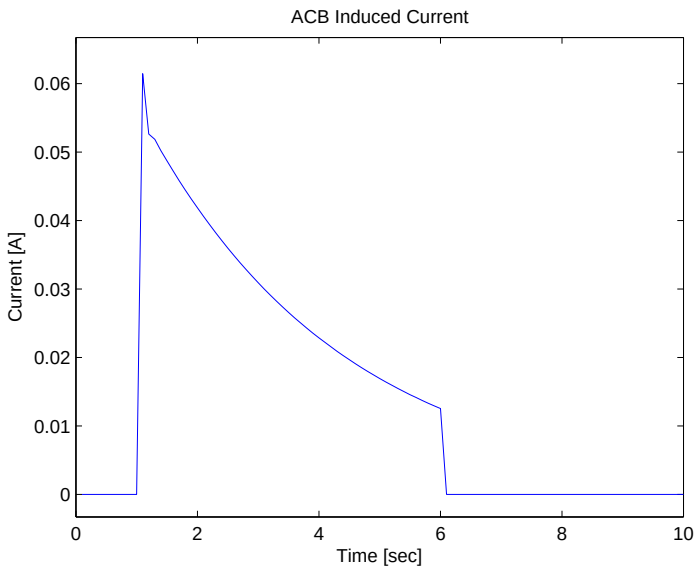

Figure 4.2: Induced current when ACB is connected to a single cell.

4.2 Charge Shuttling Between Two Series Connected Batteries

The next step of the model development was to expand the simulator to connect the ACB circuit to two electrically imbalanced batteries in series. The ACB circuit consisting of the same resistor and capacitor was used to shuttle charge from the higher voltage cell to the lower voltage cell. The balancing is done by continuously switching the balancing circuit from one battery to the other until the two imbalanced cells are balanced. This simulation was set up to observe the characteristics of the charge shuttling design between two imbalanced cells. The initial simulation was run with the switching rate of 2τ, where τ is the time constant of the ACB circuit. The time constant, given in seconds, is the product RC. The cell balancing resistor and capacitor values were again set to 100mΩ and 30F, respectively. The two series

connected batteries used the same set of second-order constant parameters with different arbitrarily selected initial SoCs; the first battery was set at 60% SoC with the other battery set at 55%. This imposes an initial voltage difference between the two battery cells.

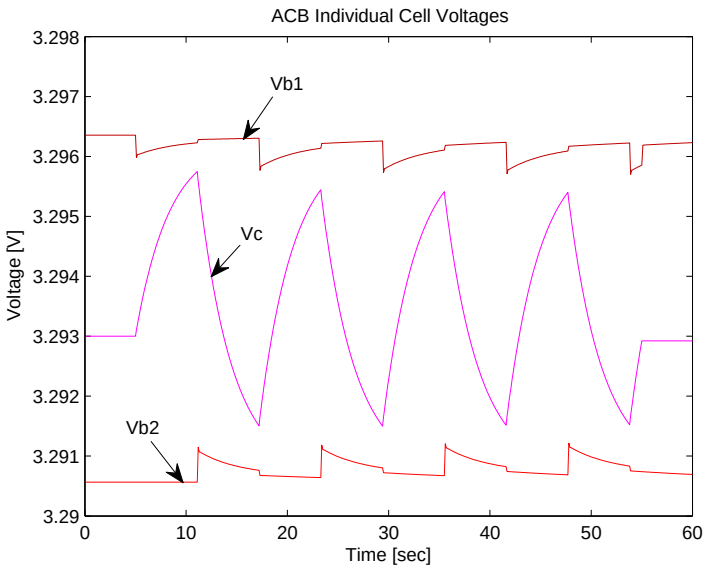

Figure 4.3: Voltage behavior when ACB circuit switches between two cells.

The simulation time was set for 60 seconds with the balancing circuit being open for the first five seconds and the last five seconds of the simulation run time. Figure 4.3 shows the voltage swing of the capacitor as it switches from one cell to the other. The capacitor removes charge from cell 1 and stores it. It then shuttles the charge by discharging it into cell 2, thus charging the battery. The same battery dynamic effects caused by the internal resistance of either battery with a sudden voltage drop can also be seen in this simulation when the ACB circuit is closed around either of the battery cells. Figure 4.4 shows the induced current in the circuit. The positive

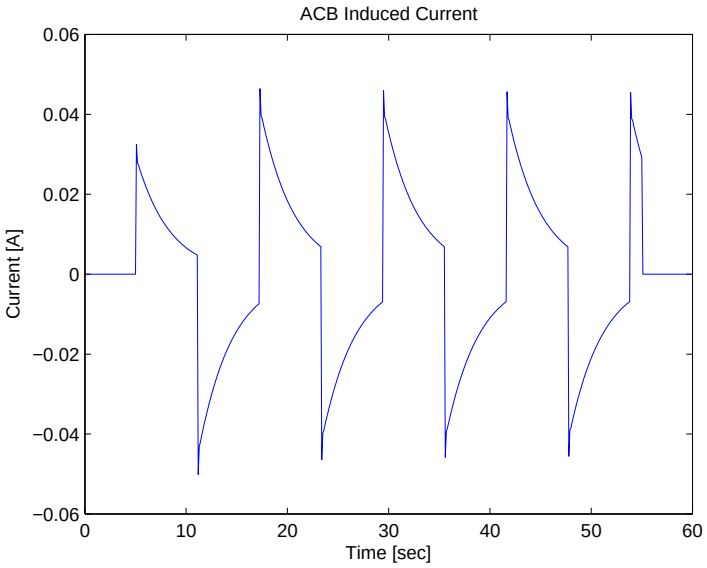

Figure 4.4: Induced current when ACB circuit switches between two cells.

currents result from the capacitor having a lower voltage than the battery to which it is connected, thus removing charge from the higher voltage cell. The negative currents occur when the capacitor has a higher voltage than the battery to which it is connected, thus delivering charge to the lower voltage cell. The current peaks progressively get smaller over time as the voltage difference between the two cells and capacitor becomes smaller.

With this simulator correctly modeling two imbalanced cells connected in series, it was used to determine the appropriate sizing for the ACB circuit components. The objective of the balancing circuit is to efficiently balance the individual cells in a pre-specified amount of time. Trends were established by simulating two series connected battery cells with an initial SoC imbalance of 10%. Numerous simulations were conducted in which the resistor, capacitor and switching frequency values of the

ACB circuit were varied while using the same set of initial battery parameters and simulation run time. The initial voltage of the capacitor was set to 3.21V and the SoC of each of the batteries was 60% and 70% for each simulation. After balancing for one hour, the energy efficiency and the SoC imbalance, shown in Figures 4.5 and 4.6 respectively, were recorded. For analysis, an energy efficiency percentage quantity, η, is defined by

$$\eta = \frac{\epsilon - \upsilon}{\epsilon} \times 100, \tag{4.1}$$

where ϵ is the total energy transferred and υ is the total energy loss through the passive elements of the circuit. These two metrics are used to determine the appropriate sizing for the ACB components to be used in this application. To evaluate the performance trends, a specific window of values was simulated for each of the components. The capacitor values range from 30F to 180F, the resistor values range from 50mΩ to 500mΩ, and the switching frequencies vary from 0.5τ to 3τ, where τ is the time constant of the ACB circuit.

The results in Figures 4.5 and 4.6 reveal that the best energy efficiencies and SoC convergence occurs with the most rapid switching frequency and the smallest resistor value. Having a smaller resistor value results in a larger balancing current and a faster balancing rate, but with the trade-off of increased energy loss. However, the efficiency of charging the capacitor in a RC circuit approaches 100% as the voltage of the capacitor approaches the voltage of the battery to which it is connected; in comparison to a capacitor that is initially discharged, a 50% efficiency is measured when completely charging it to the same voltage of the source to which it is connected [25]. The voltage differences observed in the balancing exercise for this application is on the order of millivolts; therefore extremely high efficiencies can be seen in Figure

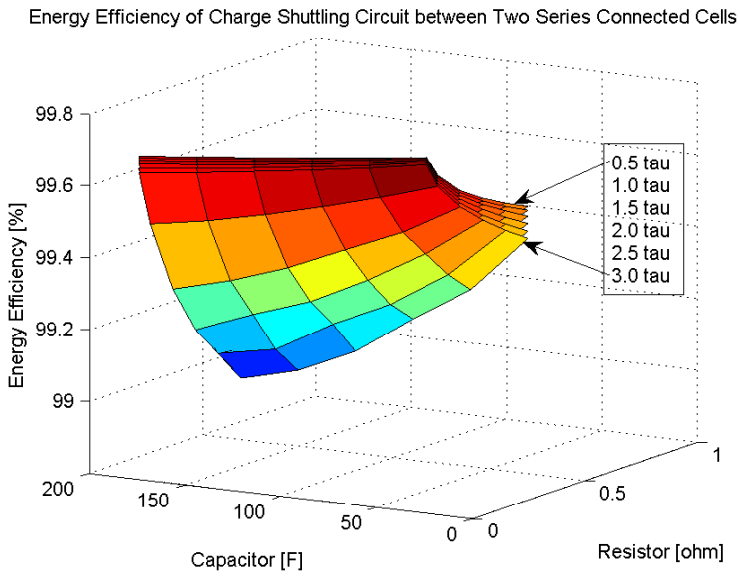

Figure 4.5: Energy Efficiency of charge shuttling circuit between two series connected batteries with an initial SoC imbalance of 10%.

4.5. This indicates that the decision of selecting components is not based on efficiency alone. Another trend, *al beit* minor, is that as the size of the capacitor increases, balancing occurs more rapidly at the cost of a slightly lower energy efficiency.

As a result of the trends seen in the ACB sizing simulations, all future simulations will be conducted with a 50mΩ resistor, a 180F capacitor and a switching frequency of 0.5τ. The upcoming sections will show that these component values will sufficiently balance a battery pack in the appropriate amount of time to meet the requirements described before for an automotive application.

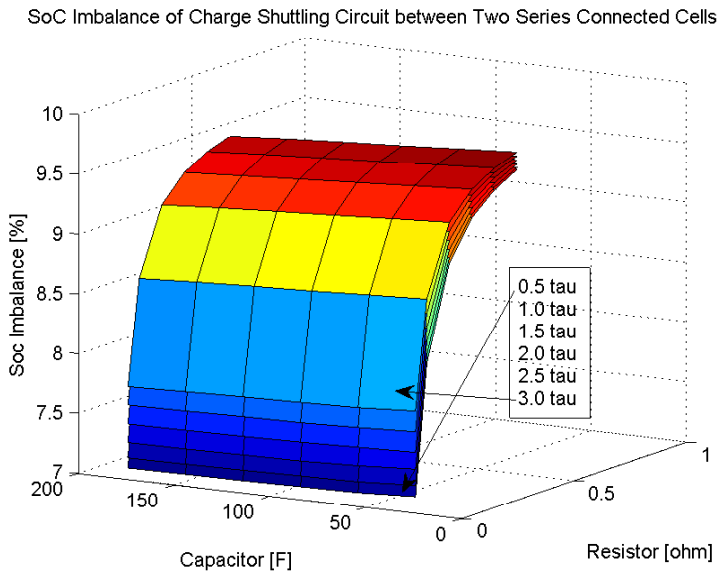

Figure 4.6: Final SoC imbalance after shuttling charge between two series connected batteries with an initial SoC imbalance of 10%.

4.3 Complete Battery Pack Simulation with ACB

The simple switching between two battery cells was used as a baseline to motivate the use of this scheme. The next step is to expand the model to switching between various battery cells in a randomly selected configuration. Since this model can be simulated for any arbitrarily selected series/parallel battery pack configuration, essentially any pack configuration can be chosen to show balancing between multiple cells. In this work, simulations will be carried out for the full battery pack with a 3P4S configuration.

The individual cell voltages are monitored to determine which cells are unbalanced. At each time step the battery cells with the maximum and minimum SoC are identified. The particular cell with the largest imbalance based on the criteria

determined from the rule-based control algorithm is isolated and connected to the ACB circuit. Charge is then shuttled from the determined battery cell with the highest voltage to the ACB capacitor. The ACB circuit then connects to the battery cell with the lowest determined voltage and shuttles charge from the capacitor to that particular cell. This switching is set to a specific frequency and the highest and lowest cells are re-identified every time step to ensure that the battery cells with the largest imbalance are the ones that are isolated for balancing with the ACB circuit. The balancing action continues until the maximum SoC deviation is less than 1.0%. Throughout the course of operation, it can be seen that the ACB circuit floats across the battery pack and connects to various cells based on the control discussed in the previous chapter.

To observe the cell balancing action in simulation, the model was set up to simulate a 15 hour rest time where the balancing circuit could operate. There is no input current profile for this simulation; the imbalance is assumed at the initial start point of the simulation. Each of the cells that comprise the 3P4S battery pack configuration used the same set of initial constant battery parameters. The ACB circuit elements were set with a resistor value of 50mΩ and a capacitor value of 180F with an initial voltage of 3.21V. To clearly show the balancing action achieved with this design, there was an initial imposed SoC imbalance set for four randomly selected cells in the battery pack and the rest were set to the same midpoint SoC. There were two extremely imbalanced cells, one overvoltaged and one undervoltaged, along with two other cells that were mildly imbalanced, again one slightly overvoltaged and the other slightly undervoltaged. The goal of this simulation was to not only show that the balancing functions correctly with two extremely imbalanced cells, but to also show

that balancing can be achieved with multiple imbalanced cells where the intelligent control actively selects the correct cell in the pack for balancing at the correct moment. Additionally, this simulation was set up to show that the time it takes to balance the cells in the battery pack is sufficient for automotive applications.

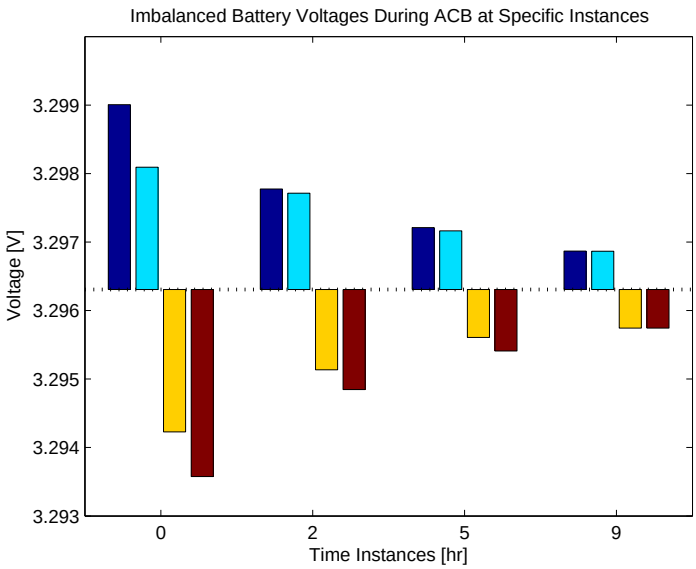

Figure 4.7: Individual cell voltages at specific time instances of the four cells with the imposed initial deviation during active balancing.

Figure 4.7 shows the voltage differences of the imbalanced cells at four specific time instances. The other individual cell voltages are not shown because they all have the same starting voltage which is at the baseline voltage, indicated in this figure by the dotted line. That is, voltages of the balanced cells vary minimally over the course of this simulation and therefore are not of specific interest. This shows over the course of time that the balancing is achieved to equalize all the voltages of the

battery pack. The complete balancing, shown in the last time instance, is achieved when the maximum SoC deviation is less than 1.0%.

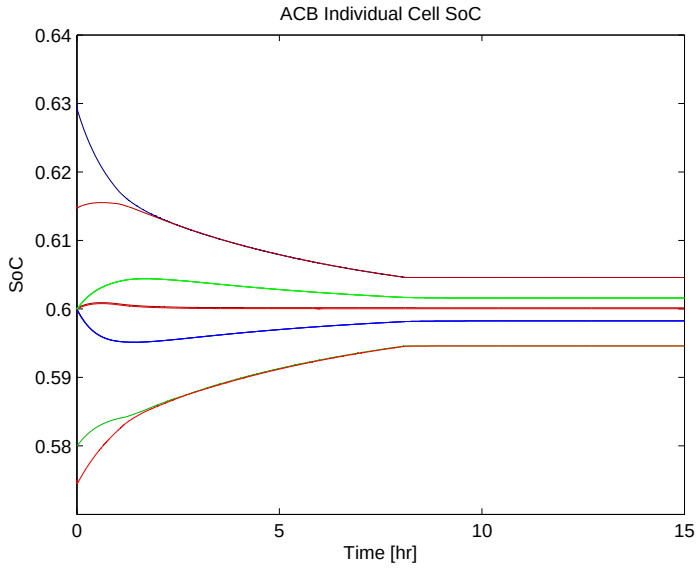

Figure 4.8: SoC curves of the individual cells with imposed deviations during ACB simulation.

Another metric used to clearly show the ACB action is to depict the behavior of the SoC curves of each individual cell in the battery pack. This metric is able to show the continuous behavior of the battery cells throughout the complete simulation run time and not just at specific time instances. Since the control continues until the SoC deviation is less than 1%, this is also a good metric to observe. Additionally, the minimal behaviors of the balanced cells in the simulation can also be observed.

Figure 4.8 shows the initial SoC imbalance, with the highest SoC set at 63%, the moderately high SoC at 61.5%, the moderately low SoC at 58% and the lowest SoC set at 57.5%. Within the first two hours of simulation, the two extremely imbalanced

cells undergo the most balancing action. It can also be seen that the other two imbalanced cells also start to become balanced. The balanced cells that had an initial SoC of 60% start to slightly drift apart. This is due to the induced current of the parallel strings caused by internal resistances of each of the cells, explained in Section 2.2. Examining Figure 4.8 further, at hour 3 that the two overvoltaged cells start to balance at the same rate and the same thing occurs for the two undervoltaged cells at hour 2. The objective of completely balancing the cells to within 1% SoC of each other was achieved in approximately 8 hours, which is sufficient for the target commuter automotive application.

4.4 Complete Battery Pack Simulation with PCB

For comparison purposes, the simulator was expanded by adding a function to simulate a passive cell balancing system for comparison with the active cell balancing method. The analytical solutions for the induced currents of the balancing were solved for and integrated into the current calculations of the system. As with the active cell balancing system, the passive cell balancing system can be simulated using any arbitrarily selected series/parallel battery pack configuration.

The passive system developed uses a shunt resistor for every battery cell in the pack as shown in Figure 3.5. As described in Section 3.5, the resistors are used to dissipate excess charge, as heat, of the cells that have a higher voltage than the balance set point voltage. The control establishes this voltage balance set point by taking the average deviation of the cells from the battery cell with the lowest voltage and adding it to that value when the battery pack is under no load input current. This works to maintain cell balancing with the particular cells that have a higher

voltage and does not dissipate any charge from the cells that have a voltage that is lower than the chosen set point. Therefore, balancing of every cell cannot be achieved in all circumstances. The individual cell voltages are monitored at each time step and balancing continues until all the battery cells with a higher voltage reach the balance voltage set point.

To observe the passive cell balancing action in simulation, the model was set up to simulate a 15 hour rest time within which the balancing circuit could operate. There is no input current profile that is set up for this simulation; the imbalance is assumed at the initial start point of the simulation and the voltage balance set point will be set once the 30 minute timer expires at the beginning of the simulation. Each of the cells that comprise the 3P4S battery pack configuration used the same set of initial constant battery parameters, except that four of the cells have different initial SoC values; two are higher and two are lower, identical to the initial set point of the simulation in the previous section. Each of the shunt resistors are 50Ω to keep the discharge current at a relatively small value of 65mA. The goal of this simulation is to not only show that the passive balancing scheme balances the higher voltage cells to the correct set point voltage, but that it also achieves the balancing in an appropriate time for automotive applications. This passive system will be used for comparison purposes with the active system in the next section.

Figure 4.9 shows the individual voltages of the four imbalanced cells at four different time instances throughout the balancing process. The baseline point shown in this figure is the voltage balancing point (dotted line) that was calculated by the controller when the rest timer expired, which is approximately 3.296V. The other cells are not shown since the voltage drifts of these cells from the voltage set point are

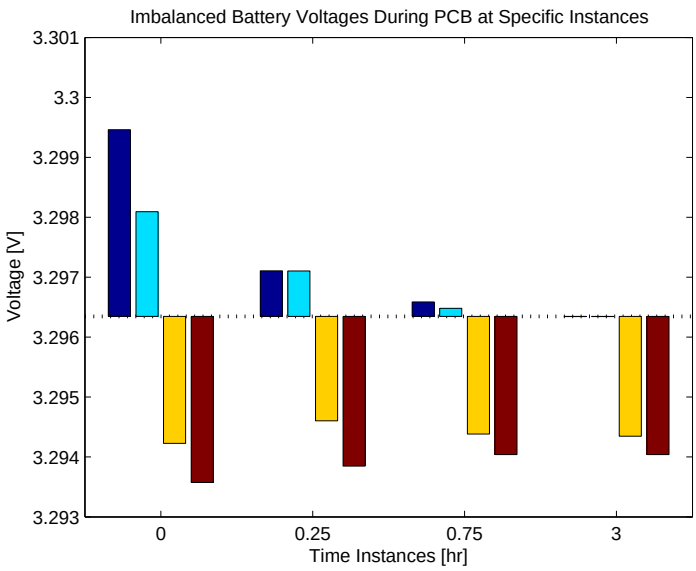

Figure 4.9: Individual cell voltages at specific time instances of the four cells with the imposed initial deviation during passive balancing.

minimal as compared to the battery cells that are depicted. The first time instance shown in this figure is that of the initial starting voltages of the simulation. The next two time instances show the voltages 15 minutes and 45 minutes, respectively, after the balancing action has started. By observing the figure, the battery cells with voltages over the set point progressively get smaller at these two time instances and the battery cells with voltages below the set point have relatively minor changes which are due to the induced currents of parallel configuration of the pack, as was explained previously. The last time instance is the final value of the battery cells after balancing has been completed, which occurs in approximately 3 hours. The balancing action only occurs on the battery cells with a voltage that is over the balancing set point. The last time instances shows that the higher battery cells are discharged to

this point. Therefore, the overall voltage deviation has been reduced by half in a relatively short time period as a result of this passive balancing scheme.

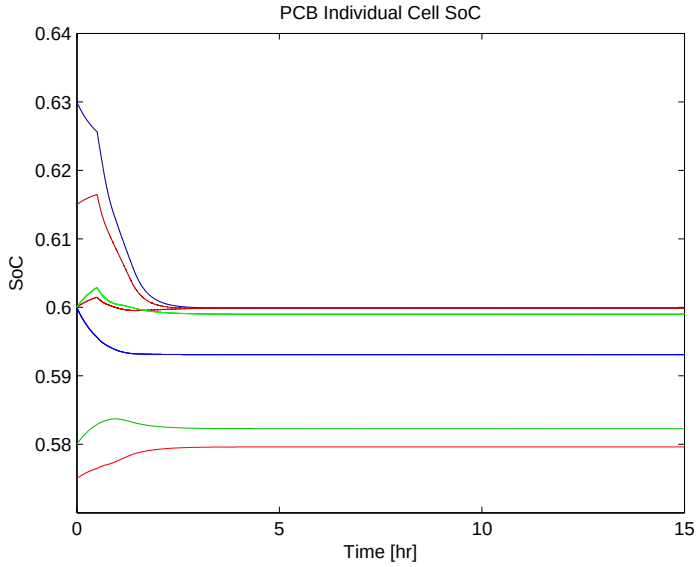

Figure 4.10: SoC curves of the individual cells with imposed deviations during PCB simulation.

The SoC curves of the entire simulation are shown in Figure 4.10. The metric is valuable in that it allows close observation of the continuous behaviors of all the individual cells in the battery pack throughout the balancing process. During the first half hour of the simulation, the normal behavior of a parallel configured battery pack can be seen in that the SoC's are drifting slightly due to the induced currents of the parallel strings caused by the differences in internal characteristics of the individual strings. At the half hour mark, the balancing timer expires, the voltage balancing is set, and the balancing system starts. Any of the individual cells that have an SoC value over 60% are balanced since the voltage at that point is approximately equal to

the set point voltage. Over the next three hours all the battery cells with high voltages are balanced to the voltage set point and it can be seen that the SoC's of these higher cells converge to a point that is near 60% SoC. The battery cells that are below this point do not undergo any balancing and simply react to the parallel string currents that are induced as a result of solving for Kirchhoff's voltage law while removing charge from the battery cells with a higher voltage. The SoC deviation reduction from 5.5% to 2% occurred over approximately three hours as a result of the passive balancing scheme.

The passive balancing scheme is a simple application for balancing battery cells in a pack. The goal is to reduce the imbalance of higher charged cells to a specific voltage set point in a certain period of time. This application has shown that it can work on parallel battery pack configurations. As seen in the previous two figures is that this balancing scheme is limited. It does nothing to balance cells that are under this voltage set point. Additionally, all the energy that is removed from the battery cells with a higher voltage is burned off as heat through the shunt resistors. The trade off of using a passive system is the relatively cheap and simple design for burning off access energy as waste heat.

4.5 Battery System Simulation Results

Now that the model with both the active and passive cell balancing has been fully developed, simulations can be run with various battery pack parameters and input current profiles. The simulator is designed to generate the base battery pack with a set of battery parameters to be used for different simulations. Multiple simulations can

then be run with both cell balancing designs on the same pack for a direct comparison of the two cell balancing systems with the base pack and with each other.

For a better representation of the individual battery cell behaviors, LPV model parameters were employed. As discussed in Section 3.6, LPV parameters provide a more realistic and accurate battery behavior representation which capture the difference in charge and discharge efficiencies over various temperatures across the SoC spectrum. In order to induce realistic scenarios, the individual battery parameters were varied, as shown in Equation 2.1, with a standard deviation of 0.015 from the base set of values. Parameter variation in this manner creates slight differences in internal resistance and overall capacity of each of the individual battery cells, which mimics manufacturing inconsistencies and relative aging, providing realistic representation of a battery module that would be seen in automotive battery packs. The variation factors for the individual battery cell internal resistance and capacity can be seen in Appendix B.

The multiple simulations conducted in this section use the same set of initial battery parameters so a direct comparison can be made. The same extended input current profile also was run in each simulation to establish initial conditions under load conditions. The current profile used for this purpose is an extended Toyota Prius HEV current profile, which is shown in Figure 4.11. This current profile is representative of a typical urban drive cycle (for example, as would be seen by a commuter in a daily trip to or from the workplace). The active drive cycle is then followed by a 12 hour rest period (presumably when the vehicle is not in service during work or overnight hours) in which the battery cells can achieve a steady-state value and may or may not be subject to a cell balancing control system.

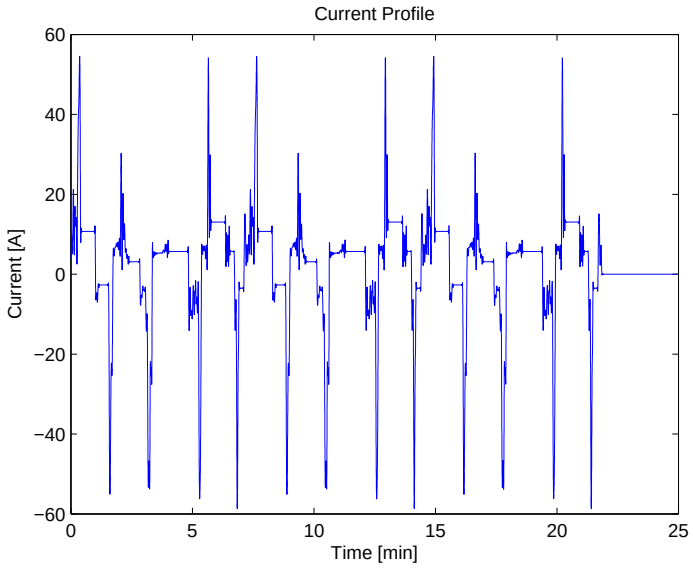

Figure 4.11: Toyota Prius extended HEV input current profile.

Therefore, the allowable time window for complete battery pack cell balancing is considered to be 12 hours. Simulations will show that the balancing can actually take less time with either balancing technique, depending on several factors in the chosen architecture and control scheme. These simulations are designed to show the voltage drift that occurs without a cell balancing system, as well as show the performance of the two proposed cell balancing designs all on the same identified battery pack.

4.5.1 Non-Balanced LPV Battery Pack Observations

All the individual batteries in this simulation hold an initial SoC value of 60%. As described before, each of the cells have unique internal resistance and capacity variations which models a more realistic battery pack configuration. The simulation was run for a 12 hour time period and Figure 4.12 shows the individual battery

voltages over the first four hours of the simulation, which also includes the active drive cycle.

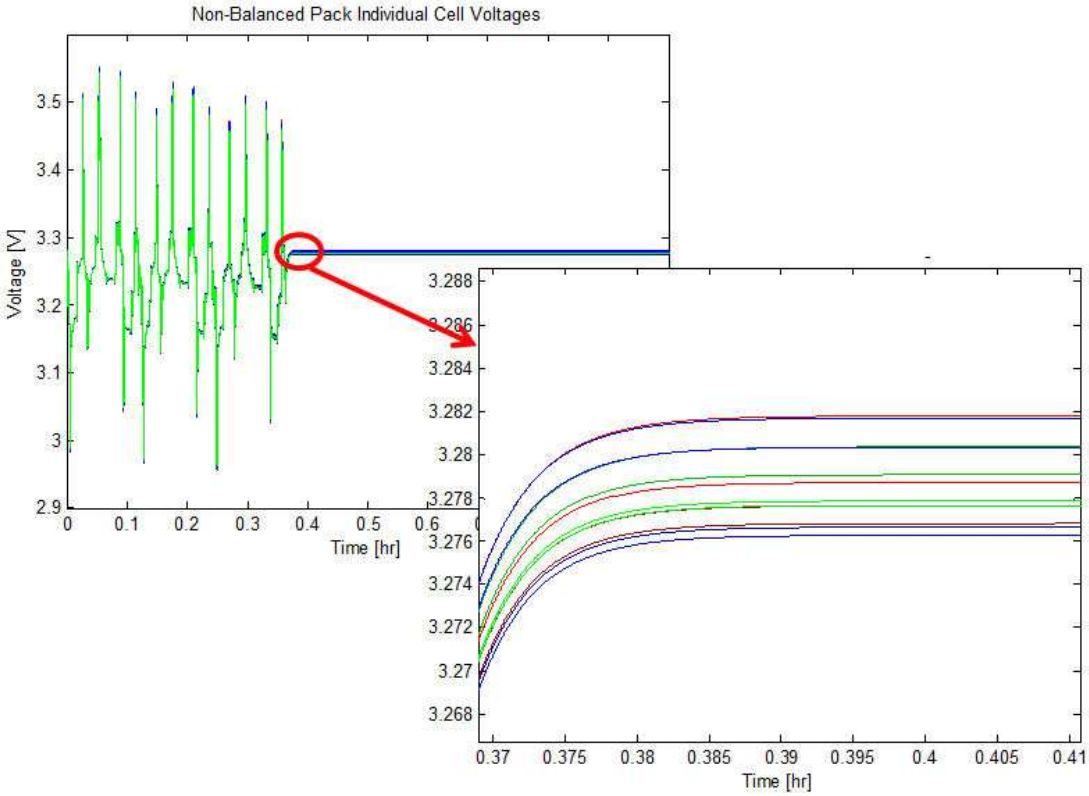

Figure 4.12: Individual cell voltages of the non-balanced battery pack.

The blow out of the individual battery voltages shown in Figure 4.12, shows the voltage drift that results from this drive cycle. The drift shown in this figure is a result of the unique variations of the individual battery cells in the pack since all the cells were initially balanced at the beginning of the simulation. The voltage drift will continue to grow as more current profiles are run on this battery pack if it is not

correctly mitigated. As the voltage drift grows, this will start to affect the operational performance of the battery pack as a whole. If the voltage of one of the cells becomes too small, it will function below its normal operating range, thus reducing the overall performance of the battery pack, and start to chemically breakdown from within.

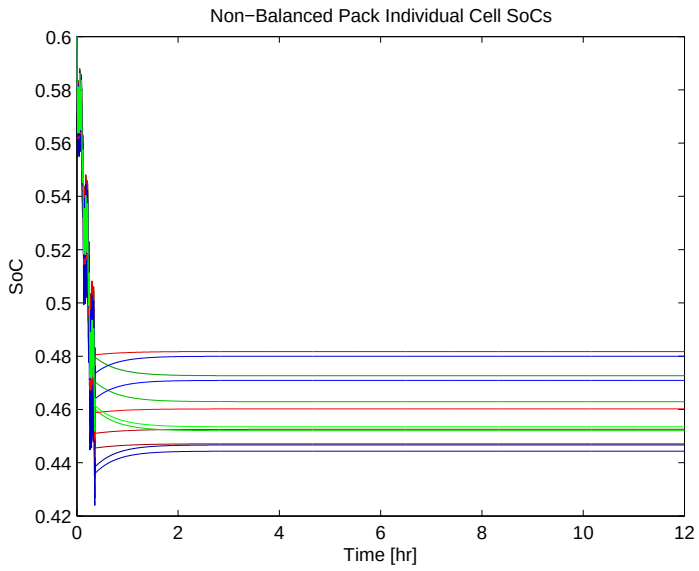

Figure 4.13: Individual cell SoC's of the non-balanced battery pack.

The voltage drift in this simulation, although rather small, when plotted across the OCV curve of the batteries, results in a large SoC deviation. The individual battery SoCs throughout the simulation are shown in Figure 4.13. The first half hour of simulation shows the individual battery SoC's behavior over the active portion of the input current profile. At the half hour mark the battery SoC's are considerably imbalanced with an SoC deviation of approximately 6.0%. Over the next hour the individual cells have a chance to relax and reach a steady-state value. The final SoC deviation over this current profile is approximately 4.0%.

This simulation, with the LPV parameters, shows a more realistic battery behavior pattern. After one cycle, it has been shown that there is a large voltage drift between the cells. As mentioned before, this will continue to grow and needs to be corrected as soon as possible to prevent battery cell degradation and reduce the expected performance and life of the battery pack. The next section will show the battery pack with the same parameters simulated with both a passive and active cell balancing system.

4.5.2 Active and Passive Cell Balancing Comparison

The battery pack with the same initial LPV parameters was simulated with both an active and a passive cell balancing system. These simulations were designed to illustrate the performance of both balancing techniques on a battery pack after being excited from a particular driving cycle. The objective of any balancing system is to establish some sort of voltage balance between the cells in the battery pack to increase expected battery performance and life span. For these simulations, the batteries in the pack were initialized with the same initial SoC of 60%, and as before the pack is simulated over a 12 hour time period. The same current profile, shown in Figure 4.11, was used to excite the batteries within the pack.

The active balancing circuit uses a 180F capacitor with an initial voltage of 3.21V and a resistor with a value of 50mΩ. The switching rate was set to 0.5τ. Figure 4.14 shows the individual cell voltages over the 90 minutes of the simulation run time. The active portion of this figure develops the voltage drift between the cells. During this time the ACB circuit is not functioning, as seen by the constant voltage of the capacitor shown in magenta. When the input current is zero, the active balancing

starts to balance the cells in the battery pack, as seen by the change in the voltage of the capacitor.

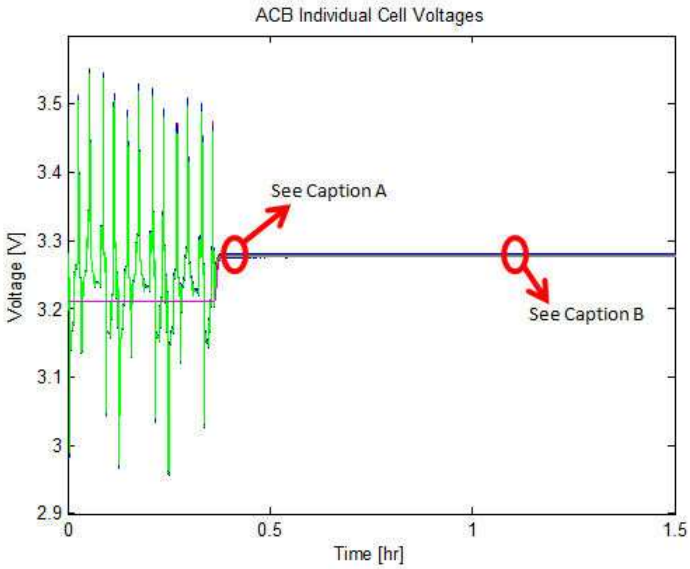

Figure 4.14: Individual cell voltages of battery pack with ACB system.
A: Switching begins between the two most imbalanced cells as shown in Figure 4.15
B: Switching between multiple cells occurs at this point as shown in Figure 4.16.

Time instance A in Figure 4.14 depicts the cell imbalance directly after the active cycle, as the balancing begins. This instance is shown more clearly in Figure 4.15. The capacitor is connected (switched) between the two cells with the highest and lowest voltage at this point. The capacitor voltage, colored magenta, increases when it is connected to the higher cell, thus removing charge from it. The capacitor voltage then decreases when it is connected to the lower cell which charges the battery cell.

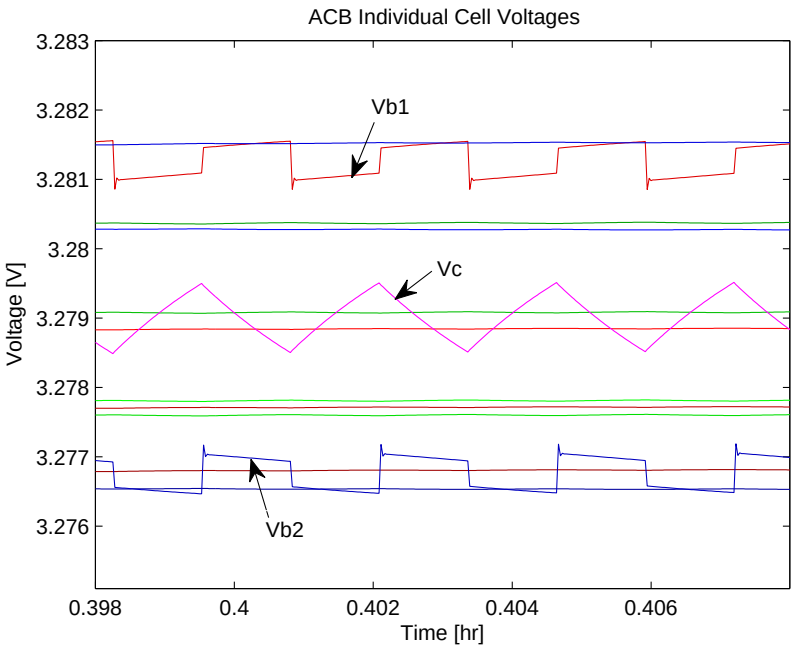

Figure 4.15: Switching begins between the two most imbalanced cells (time instance A from Figure 4.15)

Time instance B in Figure 4.14 shows the individual cell voltages after 1.3 hours of simulation time. This instance is shown more clearly in Figure 4.16. At this point, the capacitor is intelligently switching between multiple high and low voltage cells. At time instance 1.342 hours the ACB circuit is connected to a battery with a higher voltage, shown in blue, and then at time instance 1.344 hours the ACB circuit is then connected to a different cell with the highest voltage, shown in red.

The continuous SoC of the individual battery cells over the entire simulation can be seen in Figure 4.17. This clearly shows the time duration it takes to achieve the target SoC deviation of $\pm 1.0\%$ from an initial SoC deviation of 6.0% when the balancing began. This metric also provides a clearer understanding of the individual battery

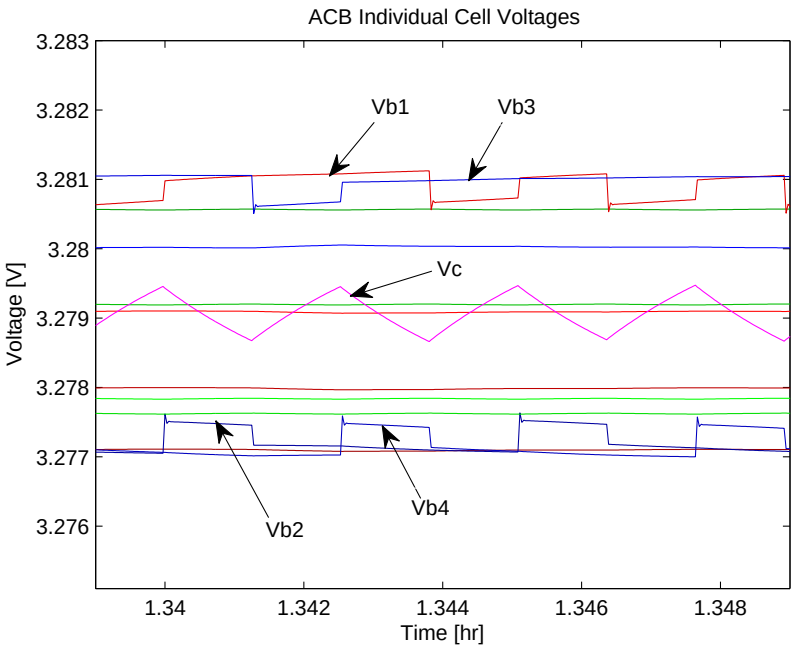

Figure 4.16: Switching between multiple cells occurs at this (time instance B from Figure 4.16)

behaviors during the balancing process. The complete balancing of the battery pack requires approximately 9.5 hours for the parameters and scheme chosen in this simulation. At hour 1.5, the balancing between multiple high and low voltage cells occurs and the balancing of these cells is completed at the same rate. This continues for the duration of the balancing process since the ACB circuit is actively switching between multiple cells. Note that because this is a charge depleting current profile, the SoC of the battery pack will be lower than its initial value. After balancing has been completed, the battery pack SoC settles to approximately 46% SoC, with all the cells within $\pm 0.5\%$ of the final value. The energy efficiency of the balancing operation as calculated by Equation 4.1 was 99.8%. Maintaining a balanced voltage of the battery

pack will allow it to operate at the expected performance level with an increased life expectancy.

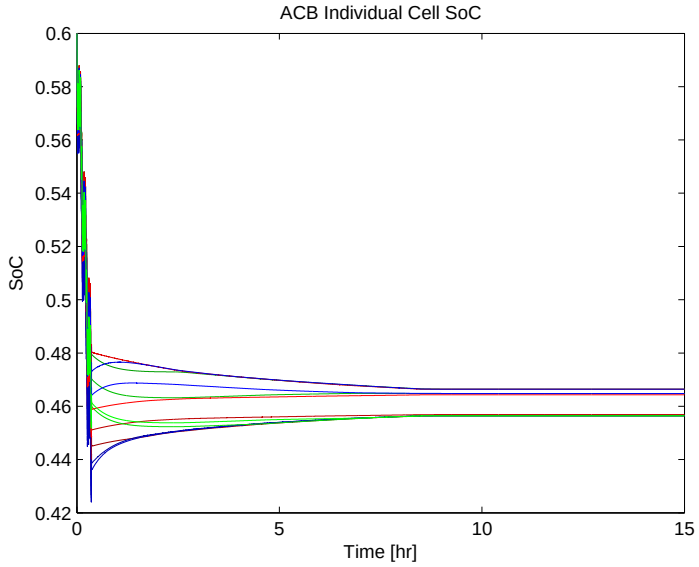

Figure 4.17: Individual cell SoC's of battery pack with ACB system.

Next, a simulation using the passive balancing scheme is investigated for the battery pack with the same individual LPV cell parameters. This passive scheme was shown to work on a battery pack with a manually selected SoC deviation in the previous section. This simulation will show the passive system performance on a battery pack with the current input profile taken off a Toyota Prius drive cycle, shown in Figure 4.11.

Figure 4.18 zooms in on the individual cell voltages during the first 90 minutes of the simulation run time. Focusing on this plot, the active portion can again be seen in the first half hour of operation. During this time the cell balancing circuit is not functioning. Once the active portion of this profile is complete (no input current) the

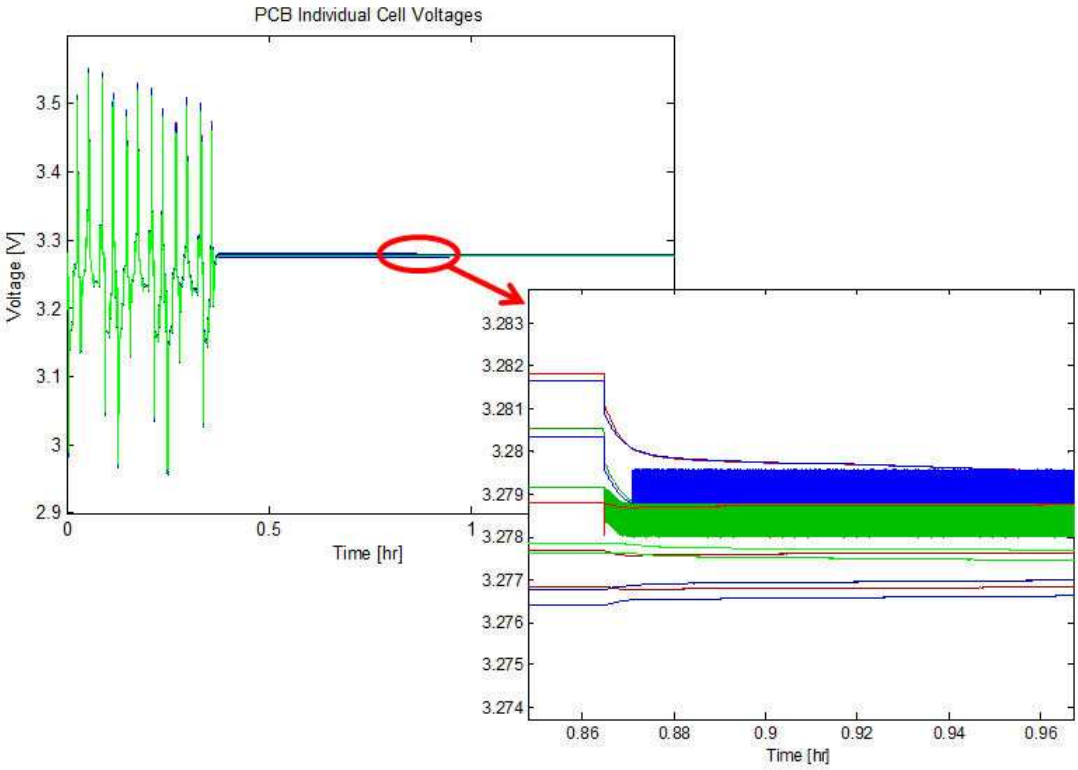

Figure 4.18: Individual cell voltages of battery pack with PCB system.

30 minute balancing timer begins. This allows the batteries to relax after having the load current removed before calculating the set point voltage for the passive balancing system. Once the timer expires, the balancing voltage set point was calculated to be 3.278V. Therefore, all the cells with a voltage that is higher than this set point are balanced by closing the respective shunt resistor circuits around those batteries to dissipate the excess energy and bring the voltages down to that set point.

The blow up shown in Figure 4.18 shows the instance that the passive systems starts operating. It can be seen in this blow out that all the cells with voltages that

are over this set point are discharged. There is also chattering that occurs, shown as large blurs in this blow up. This is caused by cells with voltages that are near this set point as the dynamic nature of connecting the battery cell to the shunt resistor causes an instantaneous voltage drop that goes below the set point. When the circuit opens, the battery voltage relaxes and raises back above the set point, thus triggering the system to balance it again. This continues until the relaxed battery cell voltage is equal to the balancing set point voltage.

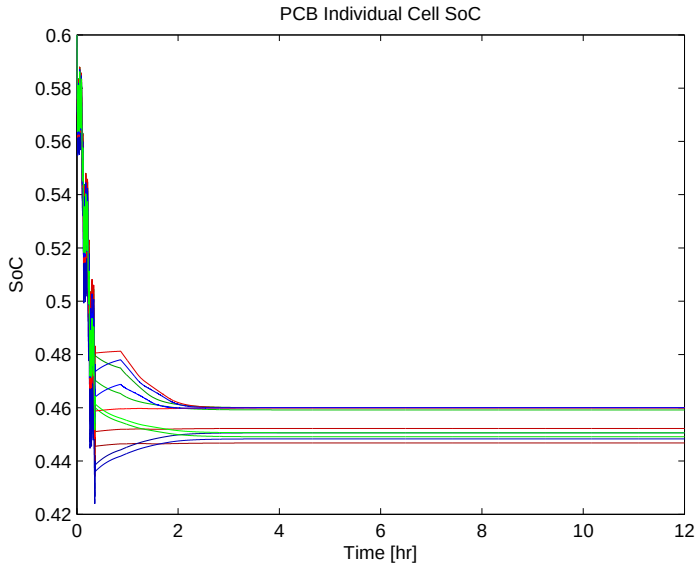

Figure 4.19: Individual cell SoC's of battery pack with PCB system.

The continuous SoC of the individual battery cells over the entire simulation can be seen in Figure 4.19. This clearly shows the duration it takes to properly balance the battery pack with the passive system from an initial SoC deviation of 6.0% when the balancing began. This metric also provides a more clear understanding of the individual battery behaviors during the passive balancing process. The batteries with

voltages are balanced to the voltage set point in approximately two hours. After balancing has been completed, the battery pack has an SoC deviation of approximately 2.0%. The higher voltage cells have balanced to approximately 46.5% SoC. The battery cells with voltages that are lower than the set point voltage are not balanced and therefore balancing of the entire pack cannot be achieved. The slight SoC drifts of the lower voltage cells seen in this experiment are caused by the induced string currents of the parallel battery pack configuration.

Since all the energy is dissipated as heat, the energy efficiency of the passive system is essentially zero. Complete balancing can be obtained if the control strategy is modified to balance to the battery with the lowest voltage. However, this will result in greater energy losses and a lower pack SoC point once balancing is complete.

A direct comparison the two balancing systems can be seen in Figures 4.20 and 4.21. The four most imbalanced cells are shown in both of the figures to show how each of the balancing systems works to achieve the goal of balancing the entire pack. When looking at the voltages, it is clear that the active system properly balances all the individual battery cells to within a certain voltage threshold whereas the passive system only balances the cells with a voltage above the calculated voltage set point. The battery cells that have a lower voltage than the rest of the pack cannot be balanced with this particular passive balancing control scheme. These lower voltages will continue to drift further away as the battery pack is continuously used and only the higher cells are balanced.

Comparing the two balancing systems from an energetics stand point, it can be seen that the active system is clearly better. With an energy efficiency of 99.8%,

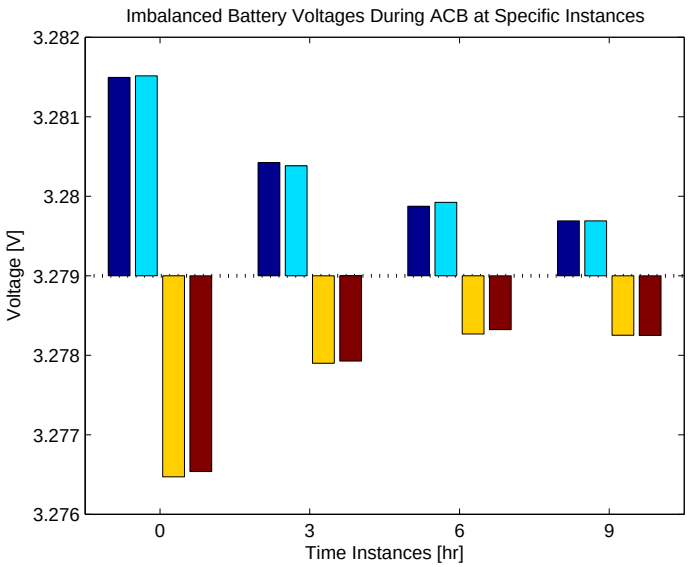

Figure 4.20: Individual cell voltages at specific time instances of the four cells with the maximum initial deviation during active balancing.

any charge that is removed from the higher voltage cells in the battery pack is essentially recovered in the battery cells with lower voltages. The passive system does have a couple of advantages. It offers faster balancing times as well as simple circuitry and control. However, the advantages of using an active balancing system are clearly shown. This design meets the specifications of a cheap and efficient method of balancing within a specific time frame for automotive applications.

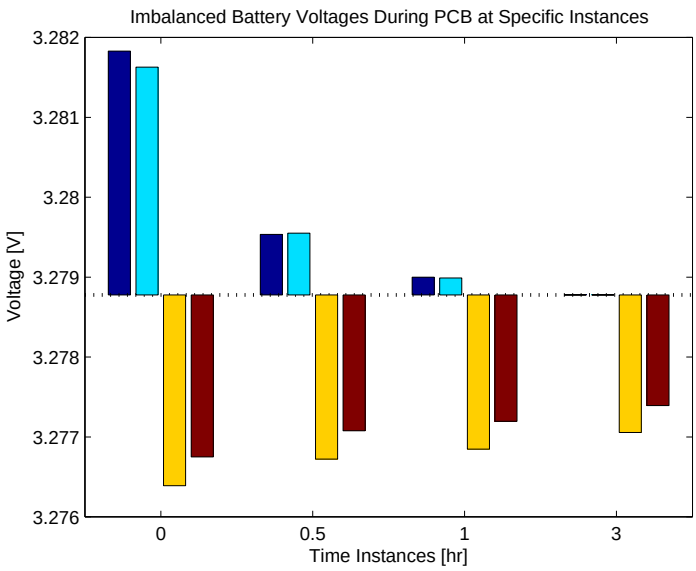

Figure 4.21: Individual cell voltages at specific time instances of the four cells with the maximum initial deviation during passive balancing.

4.6 Summary

The development of both balancing systems were described in this chapter. The simple approach of a passive system was used as a comparison for the active balancing technique. The simulation results showed that passive balancing is achieved faster but with many drawbacks that make this less appealing for larger battery packs used in automotive applications. The proposed active balancing system was shown to be a relatively cheap physical design with an efficient and timely operation based on the selected architecture and control scheme. Efficiencies of over 98% can be achieved with realistic parameters and configurations, whereas the balancing rates and efficiencies can be altered by sizing the resistor, capacitor and switching frequency differently with the active technique.

The next chapter will focus on the development of the active balancing system in experimentation. A prototype active balancing system with two imbalanced series batteries will be described for balancing scenarios similar to the simulated model. This will allow for model validation with comparing the experimental results with the simulated results. Future work will consist of various experiments to help properly build and select the components to be used for the final experimental table top battery pack.

Chapter 5

EXPERIMENTAL RESULTS OF A 12V BATTERY SYSTEM MODULE

This chapter focuses on the initial experimental results of the proposed active cell balancing technique using the "floating capacitor." The next section will examine the circuit behavior with two imbalanced cells using a manual switch which was performed in [5]. Next, an experiment with the same battery setup is performed using solid state relays for switching devices instead of a manual switch. With this experiment, the simulator model can potentially be validated by simulating the same experiment and comparing the results.

5.1 Manual Switching Between Two Series Connected Batteries

An initial experiment was conducted to show the circuit behaviors of two imbalanced series connected battery cells. The two individual battery cells that were tested are 3.2V, 2.3Ah A123 lithium-ion cells. The circuit was constructed on a breadboard. The cell balancing circuit consisted of a 58F capacitor with an ESR of 19mΩ and a 0.2Ω power resistor. The data was recorded using an NI USB-6008 DAQ. The voltages of the individual cells as well as the voltage through the capacitor were recorded. The voltage resolution was 4.88mV when using the differential analog input (AI) mode

on the DAQ. The resolution of the DAQ was not as precise as desired, but it was sufficient enough to show the dynamic behaviors of all the elements in the proposed circuit design for this experiment.

The switching in the circuit was implemented with a manual DPDT switch. The experimental test was run for 1 hour with a switching period set to 10 minutes to accurately show the circuit behaviors with two imbalanced battery cells. The initial voltage values of the batteries were arbitrarily selected and the initial capacitor voltage was set to an approximate midpoint value. The data recorded from this experiment was digitally filtered in MATLAB to clean up the signal outputs. Additionally, a voltmeter was used to manually record the initial and final voltages of the batteries and capacitor to verify the results obtained from the DAQ.

The recorded data from the experiment with the manual switching is shown in Figures 5.1 and 5.2. The ACB circuit was closed at 10 minutes and opened at 50 minutes. The switch is closed around either of the two batteries in between those times, shuttling charge from the high voltage cell to the low voltage cell. The characteristics observed here are similar to those shown in simulation from Section 4.2. When the capacitor is connected to the battery with the higher voltage, it charging occurs, thus increasing the voltage of the capacitor. When the capacitor is connected to the cell with the lower voltage, it discharges the capacitor, thus decreasing its voltage. The initial voltage drop observed in the battery behavior when connected to the circuit is caused by the dynamics and internal resistance of the cell.

Similar behaviors can also be observed when examining the current in Figure 5.2. The current spikes are the largest when the capacitor is initially connected to either one of the cells. They progressively get smaller the longer the capacitor is connected

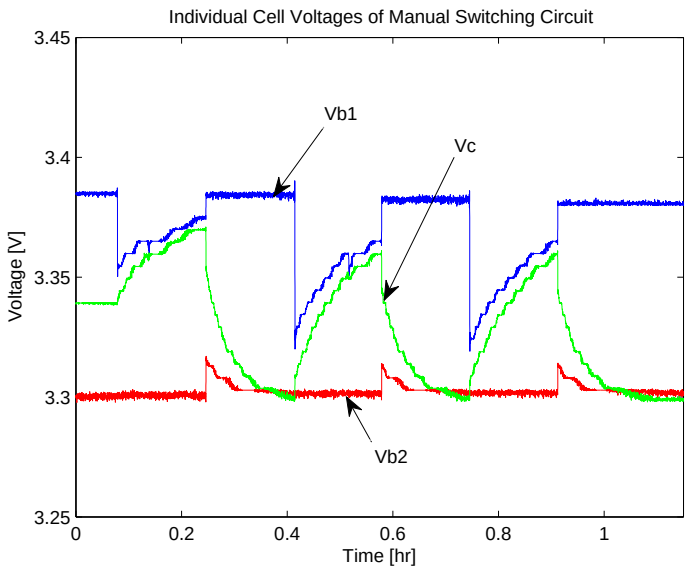

Figure 5.1: Voltage behavior with ACB circuit manually switching between two cells [5].

since the voltage difference between the cell and the capacitor becomes smaller. The positive currents are caused by the discharging of the higher voltage cell and the negative currents result from charging the lower voltage cell.

This simple experiment validated the functionality of the elements in the cell balancing circuit. The same characteristics seen in simulation can also be seen in the experimental results. As mentioned before, the initial and final voltages were recorded to verify the recorded data from the DAQ. An average OCV curve fit, shown in Figure 5.3, obtained from the experimental data obtained in [28] was used to estimate the SoC from these recorded voltages. It is confirmed that charge, *al beit* small, was shuttled from the high voltage cell to the low voltage cell during this short experiment.

Table 5.1 shows the initial and final voltages of the individual cells as well as the capacitor. Using the aforementioned second order model curve fit of the OCV,

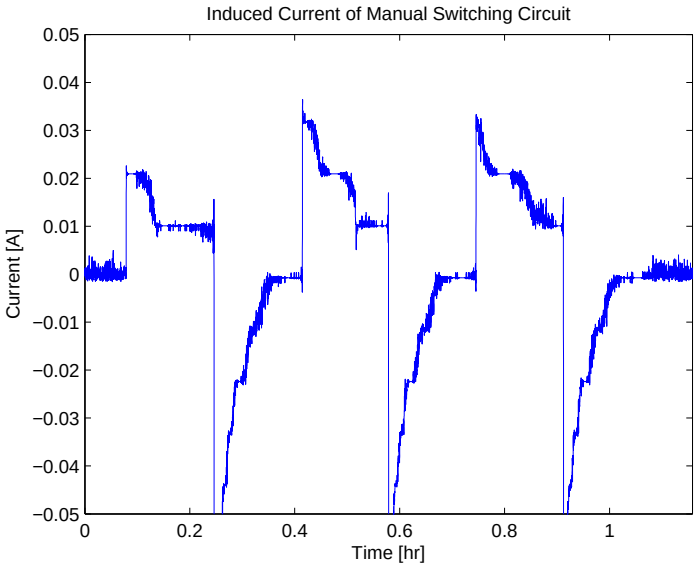

Figure 5.2: Induced current with ACB circuit manually switching between two cells [5].

an initial and final SoC difference could be calculated which is also shown in the table. This indicates that over the course of this one hour experimental test, the SoC difference decreases 0.135%. Future tests will show more accurate testing to validate the model and the functionality of the proposed system using programmable relays and a quicker balancing rate.

	Initial	Final
V_{batt1}	3.381	3.379
V_{batt2}	3.298	3.299
V_{cap}	3.339	3.299
ΔSoC	2.12%	2.05%

Table 5.1: Experimental results from manual switching.

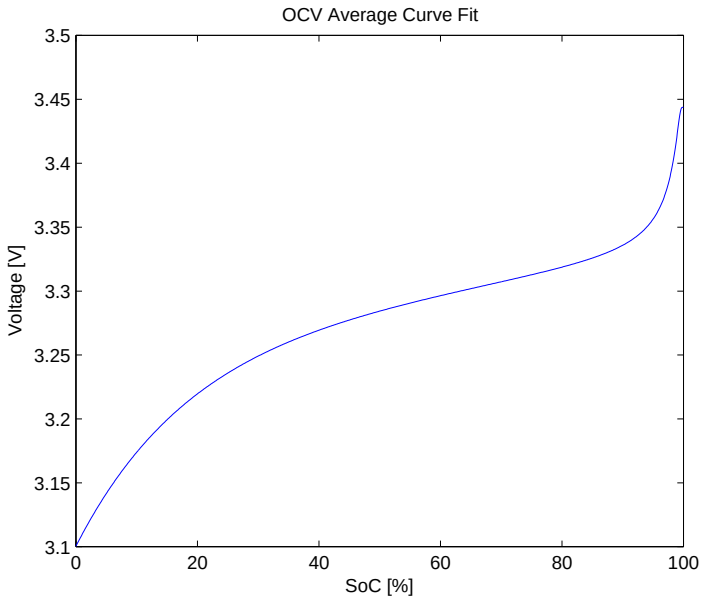

Figure 5.3: Second order model open circuit voltage curve fit.

5.2 Programmed Switching Between Two Series Connected Batteries

The manual switching circuit was then replaced with programmable solid state relays (SSRs). The SSRs used were CMX60D10 with a switch resistance of 0.018Ω. When closed, the balancing circuit consisted of two SSRs in series with a 58F capacitor around one battery cell. The total circuit resistance was calculated to be 0.055Ω, which includes the ESR of the capacitor. The new circuit was then utilized to balance the two series connected battery cells. A circuit diagram can be seen in Figure 5.4.

The control is programmed in an m-file using MATLAB. Within the script, the switching frequency and start-stop functionality is declared. The solid state relays receive a control signal from the DAQ that closes the cell balancing circuit around one of the two batteries. Two of the relays are designed to close the circuit around

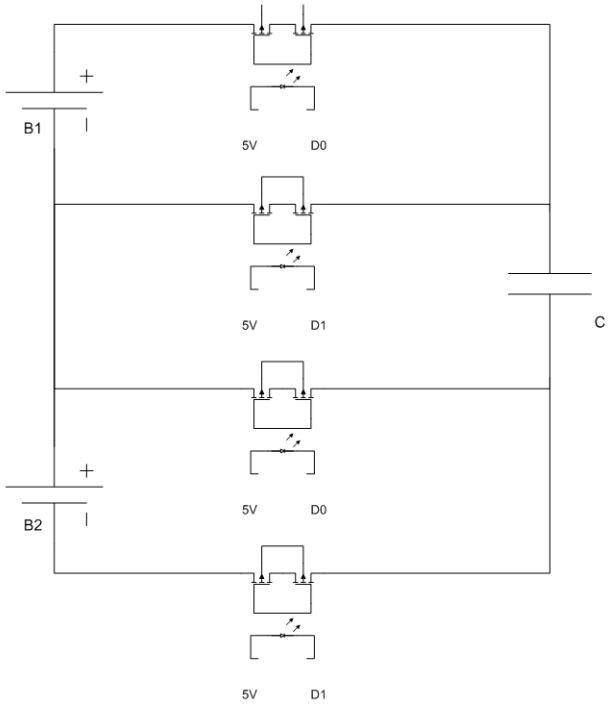

Figure 5.4: Circuit Diagram of ACB circuit using solid state relays switching between two cells.

the first cell and the other two are designed to close the circuit around the other cell. The control for the relays is programmed in a way that only one cell can be connected to the cell balancing circuit.

An experiment was conducted to correct a voltage imbalance between two series connected cells with the programmable balancing circuit. The switching frequency was set to 0.5τ and the experiment run time was set for six hours. The voltage imbalance between the two cells was set to observe the performance of the cell balancing system over the relatively flat portion in the middle of the OCV curve shown in Figure 5.3. The OCV curve was again used to estimate SoC of the individual cells based on the OCV values recorded from the voltmeter. After the six hour balancing run time,

the batteries were rested for an hour and then the voltages were again recorded. The initial and final measurements are tabulated in Table 5.2.

	Initial	Final
V_{batt1}	3.300	3.296
V_{batt2}	3.292	3.294
V_{cap}	3.296	3.296
ΔSoC	7.08%	1.57%

Table 5.2: Experimental results from SSR switching circuit.

The results in Table 5.2 indicate that charge was shuttled from the higher voltage cell to the lower voltage cell. The SoC difference was also reduced from an estimated 7.0% to 1.5%. The precision of these measurements is limited due to the limitations of the voltmeter. The accuracy of the voltmeter is 1mV, therefore the measurements may not be as precise for SoC estimation but nonetheless serves as an adequate approximation. Additionally, the voltage plot from the experimental data that was collected from the DAQ is also not accurate enough to show meaningful characteristics since the voltage measurement precision of the DAQ is 4.88mV.

However, a simulation was run in an attempt to validate the experimental results obtained. Using the developed simulator, the same test was simulated with the same initial parameters. The circuit resistance was also set to 55mΩ. The fitted SoC values from the voltage measurements were used to set the initial battery parameters in the simulation. The run time was set for seven hours with the first six enabling the active balancing and the last hour used to rest the batteries to obtain steady state values.

The individual cell voltages and the voltage of the capacitor can be seen in Figure 5.5.

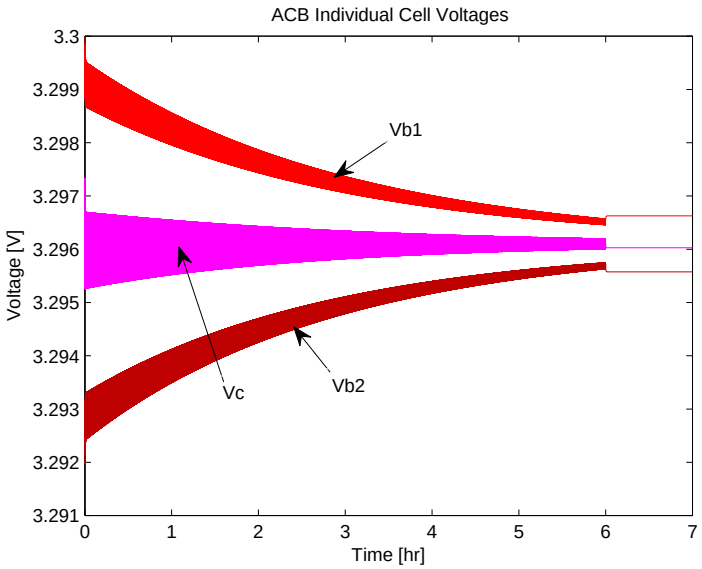

Figure 5.5: Individual cell voltages during experimental validation simulation.

By examining Figure 5.5, it can be seen that the voltage converge toward one another. The capacitor is continuously switching between the two cells, shuttling charge from the higher voltage cell to the lower voltage cell. The SoC of the individual cells can be seen in Figure 5.6. The initial SoC deviation was set to 7.08% and the final SoC deviation is just under 1.0%. The model allows for more precise voltage and SoC measurements.

Comparing the simulated results to those obtained from the experiment, it can be seen that they are relatively close to one another. The slight differences that are displayed are caused by errors in the precision of the instruments used for recording data in the experiment. Additionally, there is small a amount of leakage within the

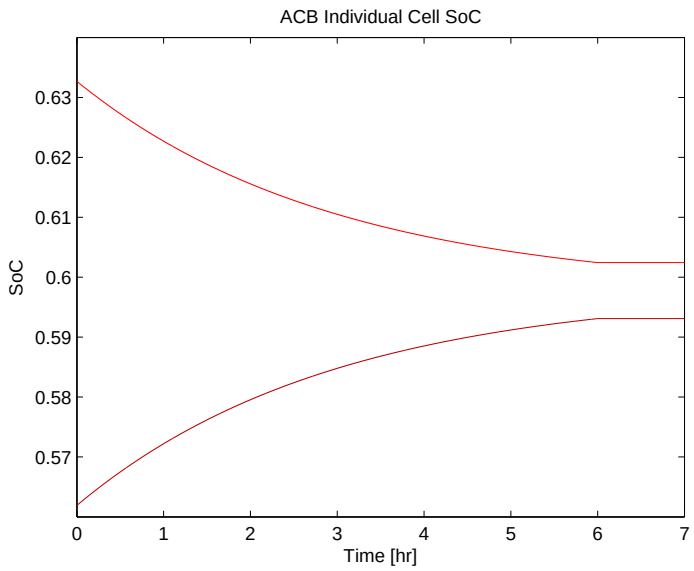

Figure 5.6: Individual cell SoCs during experimental validation simulation.

capacitor that are not accounted for. Overall, the simulated and experimental results fall within a reasonable range of each other, thus the experimental results seem to validate the results obtained from the developed simulator. Additional experiments were conducted in [5] to study the performance trends of the cell balancing circuit.

5.3 Summary

The initial experimental results of the "floating capacitor" active cell balancing method were discussed. An experiment with a manual switch was conducted to observe the characteristics of the balancing circuit. The manual switches were then replaced with programmable SSRs. The test bench was set up to run the balancing circuit on a string of two imbalanced battery cells that were connected in series. The experimental results were then tabulated and a simulation was conducted to verify the

results. When comparing the experimental and simulated results, the experimental results approximate the results obtained in simulation. Future work will include experiments to further validate the functionality of the proposed cell balancing design on a complete battery pack.

Chapter 6

CONCLUSIONS

Lithium battery packs pose significant issues with battery cell monitoring and balancing. Unlike multi-cell lead-acid battery packs, lithium-ion battery packs cannot be equalized by an overcharge, therefore a different method is required. As discussed in Chapter 1, there are two main groups of cell balancing methods: passive and active. Passive systems use a resistive element to dissipate excess energy from the cell(s) in the pack with higher voltage(s). Active balancing techniques remove excess charge from the higher voltage cells and deliver it to the cells with a lower voltage, thereby achieving cell balancing while minimizing excess energy loss as heat waste. There is very limited literature on various active cell balancing methods and due to the highly proprietary nature of the technology, there are no known commercially viable active balancing systems at a reasonable price for automotive applications.

Experimental data in Chapter 2 has shown that voltage variations within a string of series connected battery cells can occur over a relatively short amount of cycles. Simulation data has shown that voltage drifts occur quickly with parallel configured battery packs. Without mitigating these imbalances, the variations will continue to grow over continuous charge and discharge cycles. This will result in reduced battery pack performance by inducing over-voltage and under-voltage cell conditions that

will rapidly deteriorate and age the batteries, potentially leading to overheating and catastrophic failure.

Two battery cell balancing techniques were introduced in this thesis. Chapter 3 discusses these designs and a simulator was created to model the behaviors. This model was built upon previous completed research that has been conducted to identify the individual cell parameters as well as model the behaviors of an arbitrarily selected series/parallel configured battery pack. The different cell balancing circuit derivations were discussed along with the control schemes used for appropriate balancing.

The simulation results from this model were shown in Chapter 4. The step by step development of the active cell balancing method was shown in simulation. Once a complete battery pack model was developed, multiple simulations were conducted to show the effectiveness of the proposed active balancing design. Trends were examined to show how to appropriately size the active cell balancing design components for particular applications. This design was then compared to a pack with the passive balancing system as well as a battery pack with no balancing system. The comparisons were made from an effective balancing and energy efficiency standpoint.

Initial experimental results of the active cell balancing system were discussed in Chapter 5. The results provide a preliminary check on the feasibility of this design. The circuit behaviors were shown which used a manual switch to shuttle charge between two imbalanced cells connected in series. Additional experimentation provided insight to the functionality of using programmable solid state relays in the balancing circuit. The experimental results were then compared to the simulated results to validate the developed battery system model.

6.1 Contributions

An active cell balancing technique for automotive battery packs with parallel configurations has been proposed in this thesis. Much of what has been proposed in the literature focuses on series strings of batteries. With an increasing demand for more electrical capacity in new advanced vehicle architectures, more batteries will need to be placed in parallel. The proposed "floating capacitor" design is an attempt at creating a solution that is efficient, light weight, and cost effective for a parallel configured battery pack. Additionally, the developed passive balancing system in this research has provided a comparison to the active system from an energetics and feasibility standpoint. The simulated and initial experimental results have provided motivation for future work to be done on parallel battery pack cell balancing.

6.2 Future Work

The continued experimental work on the active design should be able to shed light on the implementation and practicality of the "floating capacitor" technique to actively balance cells in a parallel configured pack. The experimental results can also be used to validate the results seen from the model simulations and hopefully this will be presented in a future paper. If this method proves to be effective, it is hoped that this opens the door for more research into actively balancing parallel packs. This cell balancing scheme could also be used as part of a complete BMS in future research.

Additional advanced designs could use protected FETs in parallel with each string to drain the current from the cells that are at or near the over-voltage threshold [2]. A maintenance function could be established, with a penalty to determine the correct control pulse width modulation (PWM) for the mosfets. Potentially, a varied

resistor could instead be used with a similar maintenance function to tune the rate of balancing throughout the circuit to obtain higher efficiencies. This could then work with the established rule-based algorithm to determine a strategy using fuzzy logic control.

Appendix A

LPV BATTERY PACK SIMULATION PARAMETERS USED FOR MOTIVATION IN CHAPTER 2

	String 1	String 2	String 3
Row 1	1.0006	0.9935	0.9562
Row 2	0.9929	0.9792	0.9755
Row 3	0.9711	0.9867	0.9499
Row 4	1.0241	1.0130	0.9995

Table A.1: Capacitor variation factor for battery pack simulation.

	String 1	String 2	String 3
Row 1	1.0175	0.9487	0.9912
Row 2	0.9794	0.9606	1.0127
Row 3	1.0070	1.0008	0.9667
Row 4	1.0282	1.0088	0.9925

Table A.2: Resistor variation factor for battery pack simulation.

Appendix B

LPV BATTERY PACK SIMULATION PARAMETERS FOR CELL BALANCING COMPARISON USED IN CHAPTER 4

	String 1	String 2	String 3
Row 1	0.9893	0.9825	1.0160
Row 2	0.9898	0.9741	1.0122
Row 3	1.0216	1.0101	1.0021
Row 4	0.9871	0.9887	1.0184

Table B.1: Capacitor variation factor for battery pack simulation.

	String 1	String 2	String 3
Row 1	1.0003	1.0123	1.0105
Row 2	0.9965	0.9983	1.0019
Row 3	0.9880	0.9964	0.9987
Row 4	0.9847	1.0141	0.9830

Table B.2: Resistor variation factor for battery pack simulation.

Bibliography

[1] C. Moo, K. Ng, and Y. Hsieh, "Parallel Operation of Battery Power Modules," *IEEE Transactions on Energy Conversion*, vol. 23, June 2008.

[2] S. Moore and P. Schneider, "A Review of Cell Equalization Methods for Lithium Ion and Lithium Polymer Battery Systems," in *Proceedings of the SAE 2001 World Congress*, (Warrendale, PA, Detriot, MI), 2001. 2001-01-0959.

[3] C. Pascual and P. Krein, "Switched Capacitor System for Automatic Series Equalization," in *Proceedings of the IEEE Applied Power Electronics Conference*, pp. 848–854, 1997.

[4] I. A. GmbH, "User Manual," *Battery Control System rev. A*, 2007.

[5] Y. Chuang, "A Floating Capacitor Cell Balancing Method for Parallel Battery Modules - Final Report," submitted *The Ohio State University - ECE 783H*, Summer 2009.

[6] D. Linden and T. Reddy, *Handbook of Batteries*. McGraw-Hill, Third ed., 2002.

[7] P. Krein, "Battery Management for Maximum Performance in Plug-In Electric and Hybrid Vehicles," in *Vehicle Power and Propulsion Conference*, September 9-12, 2007.

[8] A. Taniguchi, N. Fujioka, M. Ikoma, and A. Ohta, "Development of Nickel/Metal-Hydride Batteries for EVs and HEVs," *Journal of Power Sources*, vol. 100, no. 1-2, pp. 117–124, 2001.

[9] K. Wiesener, D. Ohms, G. Benczúr-Ürmössy, B. M., and F. Haschka, "High Power Metal Hydride Bipolar Battery," *Journal of Power Sources*, vol. 84, no. 2, pp. 248–258, 1999.

[10] D. Ohms, M. Kohlhase, G. Benczúr-Ürmössy, G. Schaedlich, and K. Wiesener, "Alkaline High Power Batteries in a Bipolar Stack Design," *Journal of Power Sources*, vol. 96, no. 1, pp. 76–84, 2001.

[11] O. Bitsche and G. Gutmann, "Systems for Hybrid Cars," *Journal of Power Sources*, vol. 127, pp. 8–15, 2004.

[12] A. Affanni, A. Bellini, G. Franceschini, P. Guglielmi, and C. Tassoni, "Battery Choice and Management for New-Generation Electric Vehicles," *IEEE Transactions on Industrial Electronics*, vol. 52, October 2005.

[13] R. Spotnitz, J. Weaver, G. Yeduvaka, D. Doughty, and E. Roth, "Simulation of Abuse Tolerance of Lithium-Ion Battery Packs," *Journal of Power Sources*, vol. 163, pp. 1080–1086, 2007.

[14] A. Pesaran, "Battery Thermal Management in EVs and HEVs: Issues and Solutions," in *Advanced Automotive Battery Conference*, (Las Vegas, Nevada), February 6-8, 2001.

[15] A. Pesaran, A. Vlahinos, and S. Burch, "Thermal Performance of EV and HEV Battery Modules and Packs," in *Proceedings of the 14th International Electric Vehicle Symposium*, (Orlando, Florida), December 15-17, 1997.

[16] B. Yurkovich and Y. Guezennec, "Lithium Ion Battery Pack Model and Simulation for Automotive Applications," in *ASME Dynamic Systems and Controls Conference*, 2009.

[17] A. Baughman and M. Ferdowsi, "Double-Tiered Capacitive Shuttling Method for Balancing Series-Connected Batteries," in *Vehicle Power and Propulsion, 2005 IEEE Conference*, pp. 109–113, Sept. 2005.

[18] C. Moo, Y. Hsieh, T. I.S., and C. J.C., "Dynamic Charge Equalisation for Series-Connected Batteries," in *Electric Power Applications, IEEE Proceedings*, vol. 150, pp. 501–505, Sept. 2003.

[19] N. Kutkut, H. Weigman, D. Divan, and D. Novotny, "Charge Equalization for an Electric Vehicle Battery System," *IEEE Transactions on Aerospace and Electronic Systems*, vol. 34, pp. 235–246, Jan. 1998.

[20] Y. Lee and G. Chen, "ZCS Bi-directional DC-to-DC Converter Application in Battery Equalization for Electric Vehicles," in *IEEE Power Electronics Specialist Conference*, vol. 4, pp. 2766–2772, 2004.

[21] T. Sack, J. Tice, and R. Reynolds, "Segmented Battery Charger for High Energy 28V Lithium Ion Battery," in *The Sixteenth Annual Battery Conference on Applications and Advances*, pp. 157–159, 2001.

[22] Y. Hsieh, S. Chou, and C. Moo, "Balance Discharging for Series-Connected Batteries," in *IEEE Power Electronics Specialist Conference*, vol. 4, pp. 2697–2702, 2004.

[23] H. Park, C. Kim, G. Moon, J. Lee, and J. Oh, "Two-Stage Cell Balancing Scheme for Hybrid Electric Vehicle Lithium-Ion Battery Strings," in *Power Electronics Specialists Conference, 2007. PESC 2007, IEEE*, pp. 273–279, June 2007.

[24] Y. Lee and M. Cheng, "Intelligent Control Battery Equalization for Series Connected Lithium-Ion Battery Strings," *IEEE Transactions on Industrial Electronics*, vol. 52, October 2005.

[25] A. Baughman and M. Ferdowsi, "Double-Tiered Switched-Capacitor Battery Charge Equalization Technique," *IEEE Transactions on Industrial Electronics*, vol. 55, June 2008.

[26] J. Welsh, B. Yurkovich, S. Yurkovich, and Y. Guezennec, "A Floating Capacitor Cell Balancing Method for Parallel Battery Modules," submitted to *American Control Conference*, July 2010.

[27] B. Kuhn, G. Pitel, and P. Krein, "Electrical Properties and Equalization of Lithium-Ion Cells in Automotive Applications," in *Proceedings of the 2005 IEEE Vehicle Power and Propulsion Conference*, pp. 55–59, Sept. 7-9 2005.

[28] Y. Hu, S. Yurkovich, B. Yurkovich, and Y. Guezennec, "Battery Model Identification for HEV Applications," to appear in *IFAC Control Engineering Practice*, 2009.

[29] J. Newman, K. Thomas, H. Hafezi, and D. Wheeler, "Modeling of Lithium-ion Batteries," *Journal of Power Sources*, vol. 119, pp. 838–843, 2004.

[30] A. Ledovskikh, E. Verbitskiy, A. Ayeb, and P. Notten, "Modelling of Rechargeable NiMH Batteries," *Journal of Alloys and Compounds*, vol. 356-357, pp. 742–745, 2003.

[31] Y. Hu, "Automotive System Modeling Using Linear Parameter Varying Models," Master's thesis, Ohio State University, September 2008.